

AD _____
(Leave blank)

Award Number: W81XWH-08-1-0380

TITLE: Elucidating the Tumor Suppressive Role of SLITs in Maintaining the Basal Cell Niche

PRINCIPAL INVESTIGATOR: Lindsay Hinck

CONTRACTING ORGANIZATION: University of California
Santa Cruz, CA 95064

REPORT DATE: July 2009

TYPE OF REPORT: Annual

PREPARED FOR: U.S. Army Medical Research and Materiel Command
Fort Detrick, Maryland 21702-5012

DISTRIBUTION STATEMENT: (Check one)

Approved for public release; distribution unlimited

Distribution limited to U.S. Government agencies only;
report contains proprietary information

The views, opinions and/or findings contained in this report are those of the author(s) and should not be construed as an official Department of the Army position, policy or decision unless so designated by other documentation.

REPORT DOCUMENTATION PAGE

Form Approved
OMB No. 0704-0188

Public reporting burden for this collection of information is estimated to average 1 hour per response, including the time for reviewing instructions, searching existing data sources, gathering and maintaining the data needed, and completing and reviewing this collection of information. Send comments regarding this burden estimate or any other aspect of this collection of information, including suggestions for reducing this burden to Department of Defense, Washington Headquarters Services, Directorate for Information Operations and Reports (0704-0188), 1215 Jefferson Davis Highway, Suite 1204, Arlington, VA 22202-4302. Respondents should be aware that notwithstanding any other provision of law, no person shall be subject to any penalty for failing to comply with a collection of information if it does not display a currently valid OMB control number. **PLEASE DO NOT RETURN YOUR FORM TO THE ABOVE ADDRESS.**

1. REPORT DATE (DD-MM-YYYY) 07/31/09		2. REPORT TYPE Annual		3. DATES COVERED (From - To) 7/1/08-6/30/09	
4. TITLE AND SUBTITLE Elucidating the Tumor Suppressive Role of SLITs in Maintaining the Basal Cell Niche				5a. CONTRACT NUMBER W81XWH-08-1-0380	
				5b. GRANT NUMBER BC074170	
				5c. PROGRAM ELEMENT NUMBER	
6. AUTHOR(S) Lindsay Hinck Email: hinck@biology.ucsc.edu				5d. PROJECT NUMBER	
				5e. TASK NUMBER	
				5f. WORK UNIT NUMBER	
7. PERFORMING ORGANIZATION NAME(S) AND ADDRESS(ES) University of California MCD Biology 225 Sinsheimer Lab 1156 High Street Santa Cruz, CA 95064				8. PERFORMING ORGANIZATION REPORT NUMBER	
9. SPONSORING / MONITORING AGENCY NAME(S) AND ADDRESS(ES) U.S. Army Medical Research and Materiel Fort Detrick, Maryland 21702-5012				10. SPONSOR/MONITOR'S ACRONYM(S) Command	
				11. SPONSOR/MONITOR'S REPORT NUMBER(S)	
12. DISTRIBUTION / AVAILABILITY STATEMENT Approved for public release; distribution unlimited					
13. SUPPLEMENTARY NOTES					
14. ABSTRACT The research performed over the last twelve months is based on the hypothesis that SLIT/ROBO1 signaling regulates interactions between myoepithelial and luminal epithelial cells, and that loss of this activity results in the destabilization of the basal cell niche. We analyzed the <i>Slit2</i> ^{-/-} ; <i>Slit3</i> ^{-/-} and <i>Robo1</i> ^{-/-} null mammary gland phenotypes using a battery of immunohistochemical markers and identified discohesive, hyperplastic lesions with basal characteristics. Adhesive contacts between cells appear largely normal. The lesions have a basal character in that they contain excess basal cells, but they are not triple negative (ER-, PR-, HER2-). We performed serial transplantation of knockout tissue and discovered that the <i>Slit2</i> ^{-/-} ; <i>Slit3</i> ^{-/-} tissue displays a longevity phenotype. Mammosphere assays revealed significantly more CK8-positive cells in <i>Slit2</i> ^{-/-} ; <i>Slit3</i> ^{-/-} tissue. These data suggest that loss of <i>Slit2</i> and <i>Slit3</i> spares cell divisions along the luminal lineage, allowing the outgrowth of luminal-enriched, lateral bud structures that persist for 5-10 additional generations. Thus disruption of this basal niche, by knocking out <i>Slit2</i> and <i>Slit3</i> , results in hyperplastic lesions and deregulation of stem/progenitor cell populations. Our research promises to provide insight into the mechanisms by which normal stem/progenitor cells are regulated, leading to potential insights into how they may be deregulated upon cancerous transformation.					
15. SUBJECT TERMS breast, Slit2, Robo1, basal cell					
16. SECURITY CLASSIFICATION OF:			17. LIMITATION OF ABSTRACT UU	18. NUMBER OF PAGES 20	19a. NAME OF RESPONSIBLE PERSON USAMRMC
a. REPORT U	b. ABSTRACT U	c. THIS PAGE U			19b. TELEPHONE NUMBER (include area code)

Table of Contents

	<u>Page</u>
Introduction.....	4
Body.....	4 -9
Key Research Accomplishments.....	9
Reportable Outcomes.....	9 -10
Conclusion.....	10
References.....	10-11
Appendices.....	11-20

INTRODUCTION:

Myoepithelial cells have recently been termed the “natural tumor suppressor” of the breast because they maintain breast tissue integrity by organizing the cells in contact with them, including cells in the breast stem cell niche, located between the myoepithelial and luminal epithelial cell layers. SLITs are a family of secreted proteins that were originally identified as axon guidance cues in the nervous system. Numerous studies have demonstrated the epigenetic inactivation of *Slits* and *Robos* in multiple types of cancer, including breast, an observation supported by our studies (Marlow et al., 2008). The research we performed over the past 12 months under the auspices of an IDEA Award is based on the hypothesis that SLIT/ROBO1 signaling regulates interactions between myoepithelial and luminal epithelial cells, and that loss of this activity results in the destabilization of the basal cell niche and subsequent formation of ductal lesions with basal characteristics. Over the past 12 months, we have investigated this hypothesis as outlined in the Statement of Work by analyzing the *Slit2*^{-/-};*Slit3*^{-/-} and *Robo1*^{-/-} null mammary gland phenotypes using a battery of immunohistochemical markers. On the advice of our pathology consultant, we also performed serial transplantation of the knock-out tissue. Our data show that loss of *Slits* results in hyperplastic lesions composed of unpolarized cells. Adhesive contacts between cells appear largely normal. The lesions have a basal character in that they contain excess basal cells, but they are not triple negative (ER-, PR-, HER2-). The *Slit2*^{-/-};*Slit3*^{-/-} tissue displays a longevity phenotype that may be due to deregulation of at least one population of stem/progenitor cells.

BODY:

In initiating the work outlined in our funded application, we first considered our reviewers’ comments. Even though the application received an excellent score, the reviewers noted one minor weakness — that we did not have a pathologist examine the *Slit2*^{-/-};*Slit3*^{-/-} and *Robo1*^{-/-} lesions. To address this concern, we obtained a histopathological evaluation from Dr. Robert Cardiff who directs the UC Davis Mutant Mouse Pathology Laboratory and has extensive experience analyzing mouse models of breast cancer. As described in our funded proposal, there are extensive lesions in *Slit2*^{-/-};*Slit3*^{-/-} and *Robo1*^{-/-} glands, but they are not palpable and there is no evidence of metastasis. Dr. Cardiff described these lesions as hyperplastic and discohesive, with basal characteristics. He also described the surrounding stroma as desmoplastic and containing substantial immune infiltrates. Thus, *Slit2*^{-/-};*Slit3*^{-/-} and *Robo1*^{-/-} lesions model an early stage of breast transformation, rather than the fully transformed phenotype obtained, for example, by overexpressing MMTV-oncogenes.

Dr. Cardiff suggested we serially transplant the tissue to test whether cells are immortalized. We have established two *Slit2*^{-/-};*Slit3*^{-/-} lines; one senesced at generation 11 and the second is currently at generation 13. The contralateral wild type glands senesced, as expected, at generation 5. Lesions in the knockout outgrowths become more severe with successive transplant generations. These data, together with other data collected in the past year (see below), suggest that the observed longevity phenotype arises from a stem cell defect, and we propose to pursue the characterization of this phenotype. This will not change the scope of our research, which is focused on understanding the role of SLITs in maintaining the basal cell niche, but it will require a refinement of our technical approaches.

Outline of proposed research for the first 12 months from the Statement of Work:

*Aim I: Characterize the hyperplastic lesions observed in *Slit2*^{-/-};*Slit3*^{-/-} and *Robo1*^{-/-} mammary glands.*

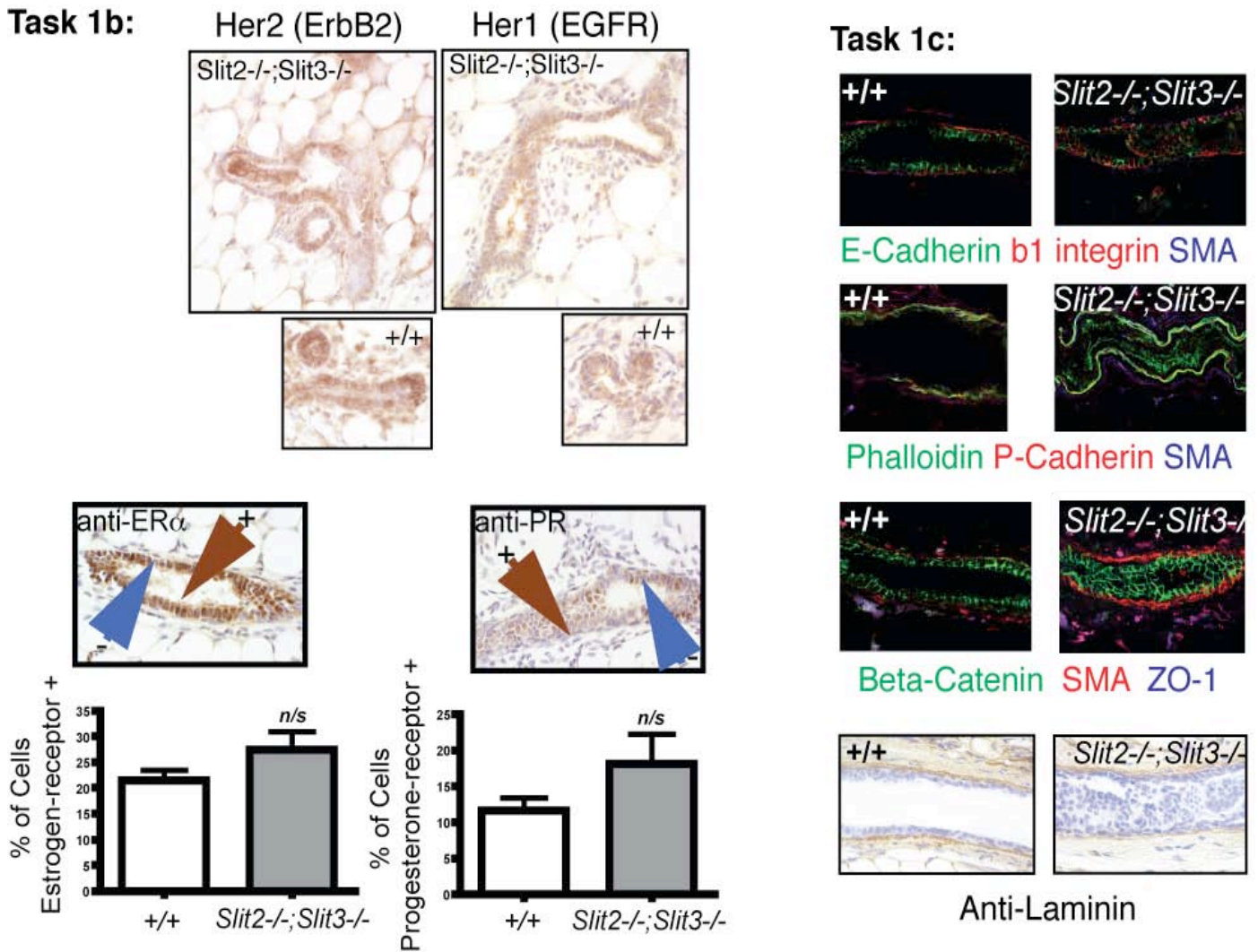
Task 1: Define the identity of the disorganized cells in ducts and document degree of polarity retained, (months 2-8)

- a. Generate tissue by transplantation

- b. Cross-section occluded ducts and double stain for CK14 (Covance) and the following markers: ER α (SCBT), HER1 (R&D), and HER2 (Chemicon) and quantify % disorganized cells with basal phenotype.
- c. Document polarity status of disorganized cells. Cross-section occluded ducts and double stain for CK14 to mark basal cells and the following polarity markers: ZO-1 (Zymed), E-cadherin (Zymed), β -catenin (SCBT), laminin (Sigma) beta1-integrin (Charles Streuli). Evaluate level of laminin staining at ductal/stromal interface and for presence in ductal lumen.
- d. Animals required: a-c) 16 immunocompromised hosts with tissue from 2 independently derived lines of tissue. Use 8 animals /fixation protocol.

Task 2: Identify the hyperproliferating cells, (months 6-12)

- a. Generate tissue by transplantation.
- b. Cross-section occluded ducts and mount alternate sections on separate slides. Double stain one set for CK14 /Ki67 and another for CK8 (DSHB) / Ki67 (SCBT). Quantify proliferative pool in each fraction



and the % basal cells in the occluded ductal space. Significance of the data will be evaluated using unpaired, two-tailed Mann-Whitney tests.

c. Animals required: a-b) 12 immunocompromised hosts with tissue from 2 independently derived lines of tissue.

Task 5: Downregulate *Robo1* expression in normal human mammary cell lines, (months 1-12)

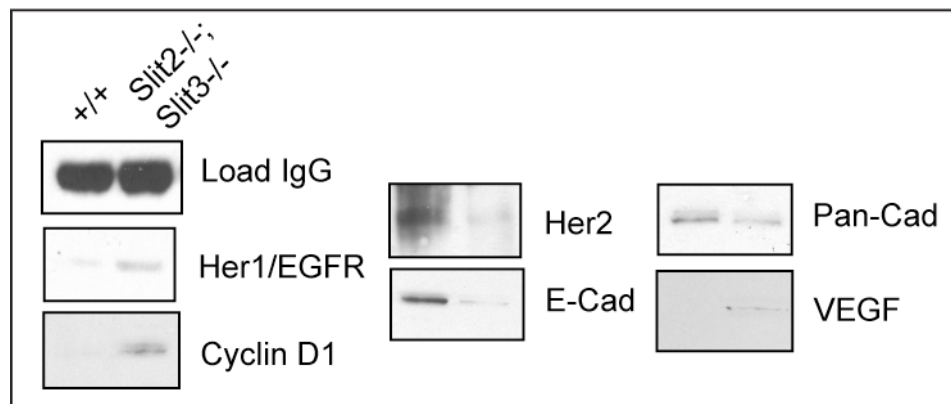
- MCF7 cells will be characterized for their expression of Slits and Robo using western blots and immunohistochemistry.
- MCF7 cells transfected with RNAi to *Robo1*(SCBT) screened for ROBO1 knockdown by Western blot (anti-DUTT1, Dr. Rabbitts) and used in Transwell and Matrigel invasion assays. Changes in migration and invasion phenotype will be quantified relative to control siRNA transfected cells. Significance of the data will be evaluated using Student's t-test.

Results and interpretations:

*Aim I: Characterize the hyperplastic lesions observed in *Slit2*^{-/-};*Slit3*^{-/-} and *Robo1*^{-/-} mammary glands.*

Task 1: Define the identity of the disorganized cells in ducts and document degree of polarity retained, (months 2-8): The basic characterization of the hyperplastic lesions observed in *Slit2*^{-/-};*Slit3*^{-/-} and *Robo1*^{-/-} mammary glands was published in October of 2008 in *Cancer Research* and the DoD was acknowledged for their support of this research. As outlined in the Statement of Work, we also performed double immunohistochemistry with CK14 and the following antibodies: Task1b -- ER α , HER1, HER2; Task 1c -- ZO-1, E-cadherin, P-cadherin, β -catenin, laminin and beta1-integrin (Figure 1). We did not see significant differences between wild type and *Slit2*^{-/-};*Slit3*^{-/-} tissue in the levels of estrogen or progesterone receptor. Analysis of cell adhesion and polarity proteins did not reveal differences in the levels of β -catenin and E-cadherin along the membrane, nor were there changes in the matrix component laminin or β -integrin. Hyperplastic cells filling the lumen appear to be unpolarized, having lost the polarity marker ZO-1 along the apical surface, although hyperplastic cells lining luminal areas appear properly polarized.

Figure 2: Immunoblotting analysis of a variety of markers. Western blots on whole gland lysates using antibodies directed against Her1/EGFR, cyclinD1, Her2, E-cadherin, Pan-cadherin, VEGF. There is an upregulation of Her1/EGFR and cyclin D1 in knockout versus ++ tissue, whereas Her2 and E-cad are downregulated.



Because these analyses did not reveal dramatic differences between wild type and *Slit2*^{-/-};*Slit3*^{-/-} tissue, we also performed immunoblotting experiments to evaluate total protein levels (Figure 2). In these analyses, we observed changes in total protein, including elevation in Her1/EGFR and, as expected in hyperproliferating cells, cyclin D1 in *Slit2*^{-/-};*Slit3*^{-/-}, compared to +/+, tissue. We also observed reductions in Her2 and E-cadherin in *Slit2*^{-/-};*Slit3*^{-/-}, compared to +/+, tissue. This later result was interesting in light of a paper, investigating

Slit/Robo1 signaling in MCF7 breast cancer cells, and showing increased E-cadherin at cell borders in cells overexpressing Slit2 (Prasad et al., 2008). Even though our immunohistochemical analysis did not reveal dramatic changes in the levels or localization of cadherin/catenin adhesion system, our immunoblotting observation in a loss-of-function setting correlates with this result of Prasad and colleagues in a gain-of-function setting. One explanation is that we may have missed, using immunohistochemistry, subtle changes in E-cadherin expression if they occurred in a subset of epithelial cells *in vivo*. Our immunoblot may have picked up this downregulation, although a caveat to the immunoblotting approach is that it was performed on whole gland, which includes adipocytes and blood vessels and, consequently, the observed changes by Western analysis may not occur within the epithelium. The ability to localize changes to the epithelium is the reason we proposed an immunohistochemical approach in our application. To investigate further, we are performing a more detailed immunohistochemical analysis to evaluate whether there are changes in the expression or localization of E-cadherin or β -catenin in a subset of *Slit2*^{-/-};*Slit3*^{-/-}, compared to +/+, mammary cells within the epithelium.

Summary Task1:

Hyperplastic lesions in the *Slit2*^{-/-};*Slit3*^{-/-} glands appear to retain many of the characteristics of +/+ tissue. The cells appear to retain relatively normal contacts, both between cells (cell-cell) and between cells and the extracellular environment (cell-ECM). Knockout cells in the middle of a lesion lose polarity, but polarity is retained when these cells are at the edge of a lumen.

Based on the recommendation of our pathologist, we performed serial transplantation analysis and discovered that *Slit2*^{-/-};*Slit3*^{-/-} glands display enhanced longevity. We have transplanted two, independently-derived lines of tissue past the usual age of senescence at generation (G) 5; one to G11 and the second, which is still growing, to G13. These aged *Slit2*^{-/-};*Slit3*^{-/-} outgrowths have a different morphology compared to younger outgrowths (Figure 3). Wild type and early generation *Slit2*^{-/-};*Slit3*^{-/-} outgrowths have ductal trees with many primary ducts arrayed in a regular branching pattern. In contrast, by G5-G10 *Slit2*^{-/-};*Slit3*^{-/-} outgrowths have only a few, short primary ducts with no formal branches, only unusual lateral bud structures.

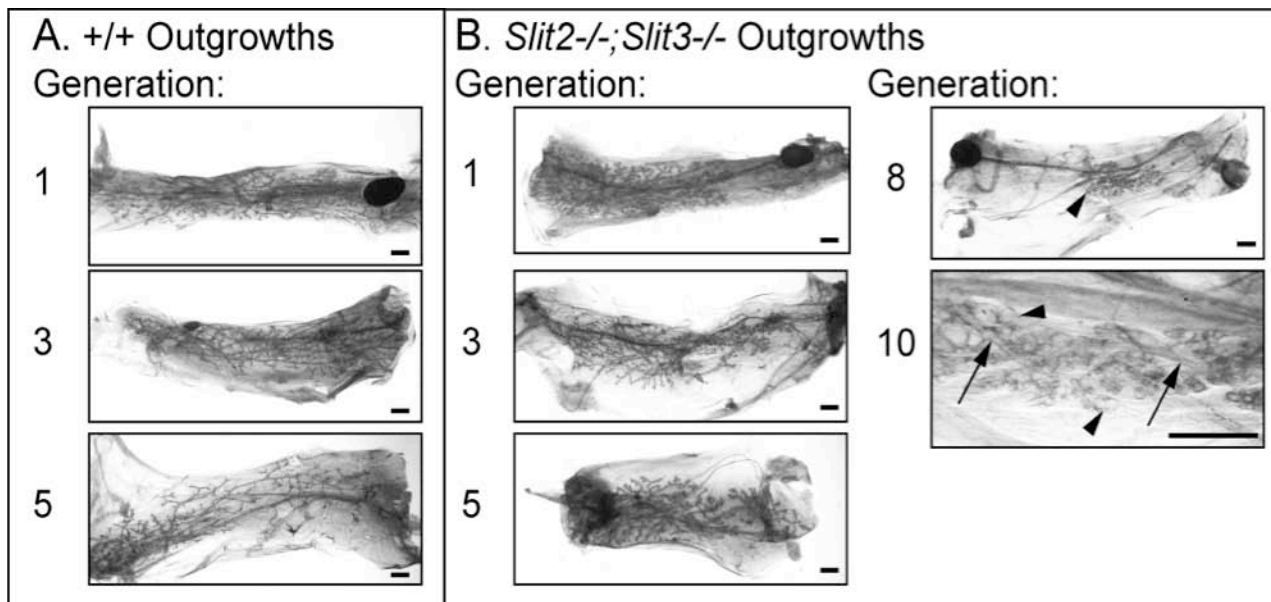


Figure 3: Whole Mounts of +/+ and *Slit2*^{-/-};*Slit3*^{-/-} Outgrowths

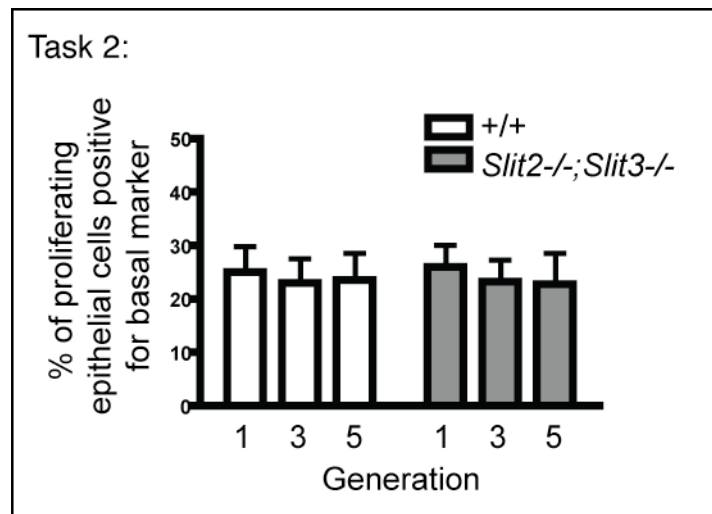
Epithelial fragments were transplanted into clear fat pads of immunocompromised mice. **A.** +/+ outgrowths senesce at G5. **B.** *Slit2*^{-/-};*Slit3*^{-/-} outgrowths senesce at G11. After G5, a change in phenotype can be seen. Arrows point to primary duct, arrowheads to lateral ductal buds. Scale bar = 1mm.

Task 2: Identify the hyperproliferating cells, (months 6-12): We performed double immunohistochemistry to identify the cells — basal or luminal — that are proliferating in tissue collected at several different transplant generations (Figure 3). We did not observe a difference in the number of proliferating basal cells between *Slit2*^{-/-};*Slit3*^{-/-} and +/+ outgrowths. Thus, even though the cells are hyperproliferating, it does not appear as if this rapid cell growth favors one population of cells over another. This indicates that both the basal and luminal cells hyperproliferate, and that the basal-like phenotype observed in the *Slit2*^{-/-};*Slit3*^{-/-} knockout is due to overall hyperproliferation of cells and not selective proliferation of the basal cell population.

To take this analysis one step further, we assessed the stem/progenitor cell populations in *Slit2*^{-/-};*Slit3*^{-/-}, compared to +/+, outgrowths by performing mammosphere assays on cells collected from different generations of outgrowths (Dontu et al., 2003) (Figure 4). Assays on G3 tissue revealed similar numbers of progenitor cells in +/+ and *Slit2*^{-/-};*Slit3*^{-/-} outgrowths. However, *Slit2*^{-/-};*Slit3*^{-/-} G5 tissue contained significantly more stem/progenitor cells compared to senescing, +/+ tissue (Fig. 4). Immunofluorescent analyses of these mammospheres revealed significantly more CK8-positive cells in *Slit2*^{-/-};*Slit3*^{-/-} tissue (Figure 5), indicating a bias toward luminal progenitors.

Figure 4: Quantification of proliferating basal cells.

Tissue sections were stained for basal and proliferation markers. The total number and double-positive cells were counted in 20 fields of view. We observe no significant difference in the number of proliferating basal cells over three generations in +/+ compared to *Slit2*^{-/-};*Slit3*^{-/-} tissue



Summary Task2:

Together, our data suggest that loss of *Slit2* and *Slit3* spares cell divisions along the luminal lineage, allowing the outgrowth of luminal-enriched, lateral bud structures that persist for 5-10 additional generations. This is an intriguing stem cell phenotype and it suggests that the hypothesis outlined in our IDEA grant is correct — that SLITs contribute in important ways to tissue integrity by maintaining and organizing the breast stem cell niche that is located between the myoepithelial and luminal epithelial layer. Disruption of this niche, by knocking out *Slit2* and *Slit3*, results in hyperplastic lesions and deregulation of stem/ progenitor cell populations.

Task 5: Downregulate *Robo1* expression in normal human mammary cell lines, (months 1-12):

These experiments were performed and published in *Cancer Research* (Marlow et al., 2008). We discovered that downregulating *Robo1* in MCF7 cells results in a hyperplastic, discohesive phenotype, similar to the phenotype observed in *Slit2*^{-/-};*Slit3*^{-/-} and *Robo1*^{-/-} mammary outgrowths.

Recommended changes in future work to better address the research topic:

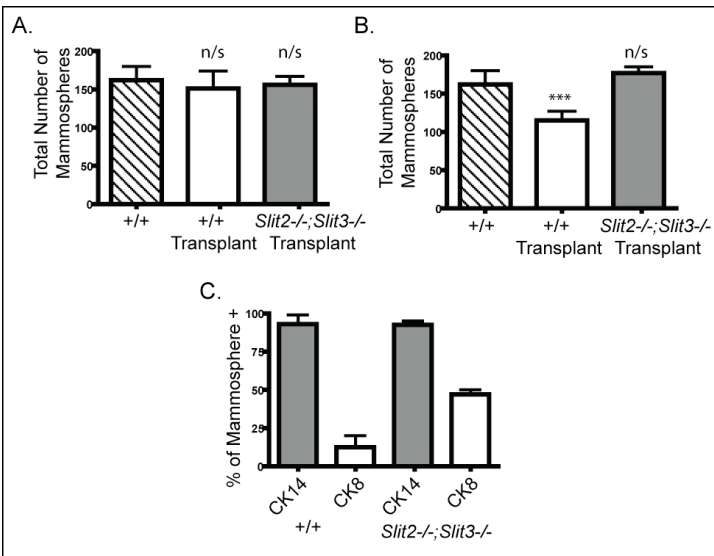


Figure 5: Mammosphere preliminary data

A. At G3 the number of mammospheres generated from +/+ and *Slit2*^{-/-};*Slit3*^{-/-} outgrowths was the same as that of +/+ intact mammary gland.

B. At G5, transplanted +/+ tissue has significantly decreased numbers of stem/progenitor cells.

C. Immunofluorescent analysis of mammospheres reveals significantly more CK8-positive cells in *Slit2*^{-/-};*Slit3*^{-/-} outgrowths, indicating a bias toward luminal progenitors .

We performed an analysis of a variety of markers, as described in the Statement of Work. However, we did not observe dramatic differences between *Slit2*^{-/-};*Slit3*^{-/-} and wild type tissue. Based on the recommendation of our pathologist, Dr. Robert Cardiff, we performed serial transplant analysis and discovered an intriguing increase in the longevity of *Slit2*^{-/-};*Slit3*^{-/-} outgrowths. This observation supports the overarching hypothesis of our Idea Award that loss of *Slits* contributes to tumor progression by disrupting stem cells that reside in the basal cell niche. We think that future effort should focus on identifying and quantifying stem cell populations in successive generations of *Slit2*^{-/-};*Slit3*^{-/-} outgrowths by mammosphere and fluorescent cell sorting assays.

KEY RESEARCH ACCOMPLISHMENTS:

- Generated *Slit2*^{-/-};*Slit3*^{-/-} and *Robo1*^{-/-} mammary glands by transplantation
- Evaluated the hyperplastic lesions in *Slit2*^{-/-};*Slit3*^{-/-} and *Robo1*^{-/-} mammary glands by performing immunohistochemical analyses using a battery of antibodies
- Published paper in *Cancer Research* identifying the tumor suppressive function of *Slits* in breast/mammary gland
- Identified a potential stem cell phenotype—increased longevity in *Slit2*^{-/-};*Slit3*^{-/-} outgrowths

REPORTABLE OUTCOMES:

Paper:

Marlow R., Strickland, P., Lee J.S., Wu X., PeBenito M., Binnewies M., Le E., Moran A., Macias H., Cardiff R.D., Sukumar S., Hinck. 2008. SLITs suppress tumor growth and microenvironment by silencing *Sdf1/Cxcr4* within breast epithelium. *Cancer Research*, Oct 1;68(19):7819-27.

Abstracts:

Rebecca Marlow, Mikhail Binnewies, Phyllis Strickland, Camilla Forsberg, Dean Li and Lindsay Hinck. Loss of *Slit* expression within the epithelium promotes angiogenesis and neoplastic transformation in breast. *Keystone Symposia: Extrinsic Control of Tumor Genesis and Progression*. March 15-20, 2009.

Rebecca Marlow, Jennifer Compton, Phyllis Strickland, Lindsay Hinck. SLIT/ROBO signalling regulates mammary gland longevity by regulating progenitor cell fate. *Mammary Gland Biology Gordon Conference*. June 14-19, 2009.

Rebecca Marlow, Mikhail Binnewies, Phyllis Strickland, Camilla Forsberg, Dean Li and Lindsay Hinck. Loss of *Slit* expression within the epithelium promotes angiogenesis and neoplastic transformation in breast. *Mammary Gland Biology Gordon Conference*. June 14-19, 2009.

CONCLUSIONS:

Evidence is growing that myoepithelial cells function as “natural tumor suppressors” because they organize tissue structure, including cells in the breast stem cell niche, and generate the barrier between epithelium and stroma by secreting the basal lamina. Over the first year of this IDEA Award, my laboratory has characterized, as outlined in the Statement of Work, the basal-like hyperplastic lesions that occur in mammary glands harboring loss-of-function mutations in *Slit2* and *Slit3*. Some of these data were published in *Cancer Research* and the rest is presented in this annual report. Evaluating a number of parameters by immunohistochemical analysis, we did not observe significant differences between *Slit2*^{-/-};*Slit3*^{-/-} and +/+ tissue. *Slit2*^{-/-};*Slit3*^{-/-} lesions express estrogen and progesterone receptors and HER2/neu at levels similar to wild type. Therefore, these lesions do not fit the triple negative (ER⁻, PR⁻, HER2⁻) classification. We did not observe significant changes in the levels and localization of E-cadherin or β -catenin within the mammary epithelium, although we are still exploring potential subtle effects of *Slit* loss on these proteins in individual cells.

Based on the advice of Dr. Cardiff, our pathologist, we made a major discovery, by performing serial transplantation assays, that loss of *Slits* results in an enhanced longevity phenotype. We previously demonstrated that loss of *Slits* destabilizes the interactions between myoepithelial and luminal cell layers --a region comprising the stem cell niche (Strickland et al., 2006). Tissue-specific stem cells are found in most, if not all, adult tissues. These cells function to fuel organ growth and regeneration throughout life. These cells are particularly important in breast which undergoes stereotyped cycles of cell growth and differentiation under the influence of estrus and pregnancy hormones. In breast tumors, the stem cell hypothesis posits that cancer stem cells, a small population of self-renewing cells within a tumor, are responsible for breast cancer progression and recurrence. This suggests that the targets of malignant transformation are normal stem/progenitor cells. Many laboratories are attempting to identify and characterize cancer stem cells. These efforts will be greatly aided by a better understanding of normal stem cells: their identification *in situ* and elucidation of their regulation during normal development. Our data suggest that SLITs regulate at least one population of stem cells. Our continued research to characterize the *Slit2*^{-/-};*Slit3*^{-/-} longevity phenotype under the auspices of the DoD promises to provide insight into the mechanisms by which normal stem/progenitor cells are regulated, leading to potential insights into how they may be deregulated upon cancerous transformation.

REFERENCES:

Dontu, G., Abdallah, W. M., Foley, J. M., Jackson, K. W., Clarke, M. F., Kawamura, M. J. and Wicha, M. S. (2003). In vitro propagation and transcriptional profiling of human mammary stem/progenitor cells. *Genes Dev* 17, 1253-70.

Marlow, R., Strickland, P., Lee, J. S., Wu, X., Pebenito, M., Binnewies, M., Le, E. K., Moran, A., Macias, H., Cardiff, R. D. et al. (2008). SLITs suppress tumor growth in vivo by silencing Sdf1/Cxcr4 within breast epithelium. *Cancer Res* 68, 7819-27.

Prasad, A., Paruchuri, V., Preet, A., Latif, F. and Ganju, R. K. (2008). Slit-2 induces a tumor-suppressive effect by regulating beta-catenin in breast cancer cells. *J Biol Chem* 283, 26624-33.

Strickland, P., Shin, G. C., Plump, A., Tessier-Lavigne, M. and Hinck, L. (2006). Slit2 and netrin 1 act synergistically as adhesive cues to generate tubular bi-layers during ductal morphogenesis. *Development* 133, 823-32.

APPENDICES:

- pdf of our paper in *Cancer Research*

SUPPORTING DATA: Figures are embedded in the text.

SLITs Suppress Tumor Growth *In vivo* by Silencing *Sdf1/Cxcr4* within Breast Epithelium

Rebecca Marlow,¹ Phyllis Strickland,¹ Ji Shin Lee,³ Xinyan Wu,³ Milana PeBenito,¹ Mikhail Binnewies,¹ Elizabeth K. Le,¹ Angel Moran,¹ Hector Macias,¹ Robert D. Cardiff,² Saraswati Sukumar,³ and Lindsay Hinck¹

¹Department of Molecular, Cell and Developmental Biology, University of California, Santa Cruz, California; ²University of California Davis Center of Comparative Medicine, Davis, California; and ³Sidney Kimmel Comprehensive Cancer Center, Johns Hopkins University School of Medicine, Baltimore, Maryland

Abstract

The genes encoding *Slits* and their *Robo* receptors are silenced in many types of cancer, including breast, suggesting a role for this signaling pathway in suppressing tumorigenesis. The molecular mechanism underlying these tumor-suppressive effects has not been delineated. Here, we show that loss of *Slits*, or their *Robo1* receptor, in murine mammary gland or human breast carcinoma cells results in coordinate up-regulation of the *Sdf1* and *Cxcr4* signaling axis, specifically within mammary epithelium. This is accompanied by hyperplastic changes in cells and desmoplastic alterations in the surrounding stroma. A similar inverse correlation between *Slit* and *Cxcr4* expression is identified in human breast tumor tissues. Furthermore, we show in a xenograft model that *Slit* overexpression down-regulates CXCR4 and dominantly suppresses tumor growth. These studies classify *Slits* as negative regulators of *Sdf1* and *Cxcr4* and identify a molecular signature in hyperplastic breast lesions that signifies inappropriate up-regulation of key prometastatic genes. [Cancer Res 2008;68(19):7819–27]

Introduction

The multistep model for breast carcinogenesis postulates that invasive carcinoma arises by way of intermediate hyperplastic lesions that progress in severity through stages of atypia to *in situ* and finally invasive carcinoma. It is generally recognized that there are clinically significant differences between various hyperplastic lesions, with some containing cellular and molecular changes that confer higher risk of progression to invasive disease. Pathologists identify clinically relevant differences later in disease progression, but early breast lesions are not well defined and further subclassification of their tumor potential by morphologic criteria is likely to be impossible. Consequently, assessing the potential risks associated with premalignant breast disease will rely on refining our understanding of the molecular signatures that confer increased risk of progression from epithelial hyperplasia to invasive carcinoma.

Up-regulation of CXCR4 is an example of one molecular change in breast cancer cells that is associated with poor prognosis (1, 2).

Its role in directing metastasizing breast cancer cells to target sites is well established (3). Little is known, however, about the role of CXCR4 during breast cancer progression, although it is up-regulated early during cellular transformation (1, 4), along with SDF1 (5), which is produced by cancer-associated fibroblasts (CAF) and is in the local environment (6, 7). Recent studies have identified roles for this signaling pathway in primary breast tumors (8, 9), and in this context, one possibility is that signaling through the CXCR4/SDF1 axis drives proliferation, conferring selective advantage to cells as they transform into metastasizing carcinomas. Several mechanisms up-regulate CXCR4 during tumor metastasis (10–13), but there is little information about mechanisms regulating the SDF1/CXCR4 chemokine axis in organs at early stages of transformation.

SLITs (*Slit1*, *Slit2*, and *Slit3*) are a family of secreted proteins that mediate positional interactions between cells and their environment during development by signaling through ROBO receptors (*Robo1*, *Robo2*, *Robo3*, and *Robo4*; ref. 14). SLIT/ROBO signaling, however, is not restricted to development, and loss of these cues likely plays an important role during tumor progression. *Slits* and *Robos* are considered candidate tumor suppressor genes because their promoters are frequently hypermethylated in epithelial cancers (15–18). In ~50% of sampled human breast tumors, *Slit2* or *Slit3* gene expression is silenced (15, 19).

Cross-talk between SLIT/ROBO and CXCR4/SDF1 signaling has been observed in several systems, with the regulatory effect occurring downstream of the receptors and involving modulation of intracellular signaling intermediates. In leukocytes and human breast cancer cell lines, SLIT impedes SDF1-induced chemotaxis (20, 21). In breast cancer cells, this deterring effect occurs via SLIT-mediated inhibition of SDF1-induced activation of signaling pathways involved in motility (21). Similarly, in the nervous system, a reciprocal regulation of SLIT-mediated axonal repulsion by SDF1 is exerted through modulation of cyclic nucleotide signaling intermediates (22). These studies show an intriguing interrelationship between these signaling axes but do not address the consequences of losing the function of one of these signaling systems, such as occurs in breast during tumor progression when *Slit* expression is silenced.

Here, we investigate the consequences of losing SLIT/ROBO1 signaling in murine mammary gland, human breast cancer cells, and human tumors. We identify *Sdf1* and *Cxcr4* as critical targets of SLIT/ROBO1 regulation. Exploiting the ability to transplant knockout mammary epithelium into host mammary fat pads, we determine the compartment, epithelial or stromal, in which SLIT/ROBO1 signaling occurs, and how loss of signaling in one location leads to alterations across the epithelial/stromal boundary. Finally, we explore the tumor-suppressive capabilities of *Slits* using a xenograft model of human breast cancer.

Note: Supplementary data for this article are available at Cancer Research Online (<http://cancerres.aacrjournals.org/>).

R. Marlow and P. Strickland contributed equally to this work.

Requests for reprints: Lindsay Hinck, Department of Molecular, Cell and Developmental Biology, University of California, Santa Cruz, CA 95064. Phone: 831-459-5253; Fax: 831-459-3139; E-mail: hinck@biology.ucsc.edu.

©2008 American Association for Cancer Research.

doi:10.1158/0008-5472.CAN-08-1357

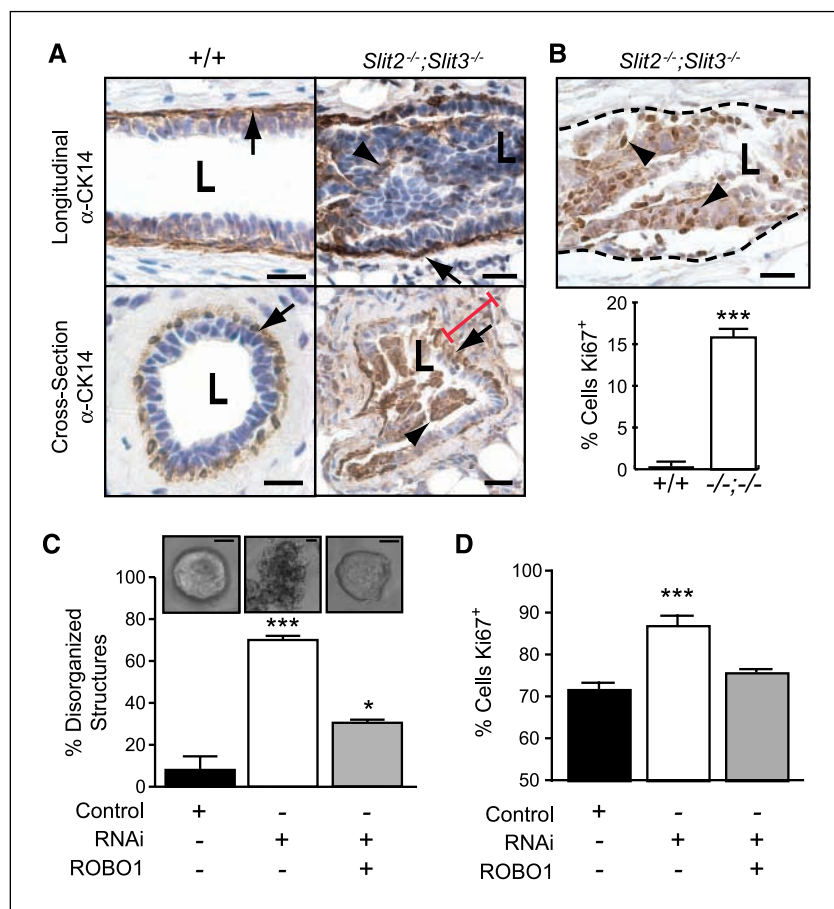


Figure 1. Loss of *Slit2* and *Slit3* expression in mammary epithelium leads to the formation of hyperplastic disorganized lesions. **A**, lack of SLIT in the epithelium leads to lesion formation. Immunostaining with anti-CK14 on longitudinal sections and cross-sections through +/+ and *Slit2*^{-/-};*Slit3*^{-/-} mammary outgrowths. Arrows, ductal myoepithelial cell layer; arrowheads, CK14-positive cells abnormally located in the lumen. **L**, lumen. **B**, lack of SLIT leads to hyperplasia. Representative lesion with dashed line indicating epithelial/stromal interface. Arrowheads, Ki67⁺ cells. Columns, mean percentage [$n = 3$ animals at 12 wk of age, 15 fields of view/animal (5 \times); bars, SD. ***, $P < 0.0001$, unpaired t test. **C**, lack of ROBO1 leads to a disorganized phenotype in three-dimensional culture. After transfection, MCF7 cells were grown in Matrigel. After 5 d, colonies were photographed (5 \times) and percentage of disorganized structures was counted. Representative images of colonies are shown. Scale bar, 10 μ m. Columns, mean percentage; bars, SD. ***, $P < 0.0001$, ANOVA. **D**, lack of ROBO1 increases the cell proliferation index. Columns, mean percentage of Ki67⁺ cells; bars, SD. **, $P < 0.001$, ANOVA.

Materials and Methods

Clinical samples. Frozen or formalin-fixed paraffin-embedded tissue specimens were collected at Johns Hopkins University (Baltimore, MD). All human tissue was collected using protocols approved by the Institutional Review Board. Informed consent was obtained from each individual who provided tissue linked with clinical data.

Animals. The study conformed to guidelines set by University of California at Santa Cruz animal care committee (Chancellor's Animal Research Committee). Mouse *Slit2*, *Slit3*, and *Robo1* nulls were generated and genotyped as described (23).

Transplant techniques. Mammary anlage was rescued from E16-20 embryos and transplanted into precleared fat pads of athymic nude mice (24). Tissue fragments from the resulting outgrowths were contralaterally transplanted to generate knockout and wild-type tissue controls (25).

Implantation of Elvax beads. Elvax, an ethylene vinyl copolymer capable of sustained slow release of bioactive molecules, was prepared as described (26), with pellets containing 225 ng SDF1 and 0.45 mg bovine serum albumin (BSA) for control. Pellets were contralaterally implanted into the fat pad of wild-type CD1 mice ($n = 3$), and tissue was harvested after 6 d.

Cell lines, DNA constructs, and antibodies. MCF7 and MDA-MB-231 cells were maintained in DMEM supplemented with 10% FCS. pGL-CXCR4(-375) contains CXCR4 between -357 and +51 relative to the transcription site followed by the luciferase gene (12). pCRII-SDF1 (for riboprobes) contains 538-nucleotide fragment of the mouse *Sdf1* cDNA (27). Mouse image clone 3385804 (American Type Culture Collection). Small interfering RNA (siRNA) directed against *Robo1* was from Santa Cruz Biotechnology. pSecTagB-*hSlit3*-C-myc was from Dr. Roy Bicknell (University of Birmingham, Birmingham, United Kingdom). The following antibodies were used: anti-CK14 (AF64, Covance), anti-SMA (1A4, Sigma),

anti-Ki67 (Santa Cruz Biotechnology), anti-CXCR4 (Abcam), anti-SDF1 (Santa Cruz Biotechnology), anti-SLIT3 (Chemicon), anti-SLIT2 (Chemicon), anti-HAL (Dr. Doug Kellog, University of California, Santa Cruz, CA), anti-Myc (9E10), anti-ROBO1 (Abcam), and anti-extracellular signal-regulated kinase (Santa Cruz Biotechnology).

Generation of stable cell lines. MDA-MB-231 cells were transfected with pSecTagB-Slit2-HA and pSecTagB-Slit3-Myc and selected in zeocin (Invitrogen). $n = 3$ lines were generated expressing SLIT2-HA and $n = 2$ lines expressing SLIT3-Myc.

Tumor generation. Stable cell lines (10^6 cells) were injected into precleared fat pads of nude mice. Tumor volume was calculated using the formula $(\text{length} \times \text{width})^2/2$.

Immunohistochemistry. Tissue was fixed in 4% paraformaldehyde. Paraffin-embedded tissue was sectioned at 6 μ m and serially mounted. Standard protocols were used and avidin-biotin complex method (Vector Labs) was used for amplification.

Scoring of immunohistochemistry. Immunostaining was scored according to percentage positive cells (P) and staining intensity (I). Score equals $P + I$. P scores 0 (none), 1 (<1%), 2 (1-10%), 3 (10-30%), 4 (30-60%), and 5 (>60%). I scores 0 (none), 1 (weak), 2 (intermediate), and 3 (strong).

siRNA transfection. MCF7 cells were transiently transfected using *Robo1* siRNA (Santa Cruz Biotechnology) and Lipofectamine 2000 (Invitrogen) according to the manufacturers' instructions. For three-dimensional culture, the "on-top" method was used (28). For luciferase assay, 48 h before harvest, cells were cotransfected with pGL-CXCR4(-375) (F-luciferase) and pRL-TK (R-luciferase). Cells were lysed using passive lysis buffer and assay was carried out in triplicate using the Dual-Luciferase Assay System (Promega) and Wallac Victor Luminometer (Perkin-Elmer Life Sciences) according to the manufacturers' instructions. F-luciferase activity was normalized to R-luciferase activity (transfection efficiency).

Western blotting. Western blotting was performed using standard procedures (29). Band intensity was scanned using Typhoon 9410 imager and quantified using ImageQuant 5 software.

Quantitative real-time reverse transcription-PCR analysis. Real-time reverse transcription-PCR (RT-PCR) analysis was done as previously described (30). Data were first analyzed using the Sequence Detector Software SDS 2.0 (Applied Biosystems). Results were calculated and normalized relative to glyceraldehyde-3-phosphate dehydrogenase (GAPDH) control. All of the PCR assays were done in triplicate, and mean values are shown in figures.

In situ hybridization. *In situ* hybridization was carried out as described previously (23, 25).

Primary cell isolation. Primary mammary epithelial cells were prepared from mild collagenase and dispase digestion, as described (23). Cells were plated overnight and then trypsinized and placed onto Matrigel-coated coverslips.

Chemotaxis assay. Chemotaxis was examined as described before (29). Phase-contrast images were acquired at 0 and 60 min. The change in cell area in the directed quadrant was calculated using ImageJ.

Statistical analysis. We used factorial design ANOVA, unpaired *t* tests, or Mann-Whitney tests to analyze data as appropriate. Significant ANOVA values were subsequently subjected to post-test using the Tukey-Kramer comparison. We report *P* values for each statistical test; all *P* values were <0.05.

Results

Loss of *Slit* or *Robo1* in mammary epithelium leads to the formation of hyperplastic, disorganized lesions. Given the

expanding role of SLITs in epithelial biology, we hypothesized a tumor-suppressive function for *Slits* in breast. We previously showed that two *Slit* family members, *Slit2* and *Slit3*, are expressed in murine mammary gland (23). The homozygous *Slit2*^{-/-} mutation causes perinatal lethality. Therefore, to investigate the consequence of its loss in mature mammary gland, we generated *Slit2*^{-/-};*Slit3*^{-/-} outgrowths by contralateral transplantation of knockout and wild-type anlage into cleared fat pads of immunocompromised mice (24).

We examined mature *Slit2*^{-/-};*Slit3*^{-/-} mammary outgrowths for morphology. Compared with the open lumens and organized bilayers of ducts in control outgrowths, *Slit2*^{-/-};*Slit3*^{-/-} ducts displayed striking abnormalities (Fig. 1A). The phenotype was 100% penetrant, with ~30% of ducts having lesions extending between 0.3 and 5.0 mm. We categorized the lesions as mild and severe. Mild lesions contained cells in the luminal space (10.1% ± SE 1.9; *n* = 621 ducts; 5 outgrowths), and many of these cells were peeled away from the myoepithelial layer, similar to an adhesive defect previously described in *Ntn1*^{-/-};*Slit2*^{-/-} glands (23). In severe lesions (17.8% ± SE 8.1; *n* = 621 ducts; 5 outgrowths), ductal lumens were occluded with a disorganized mass of cells (Fig. 1A). These excess cells suggested disrupted growth control due to either increased proliferation and/or decreased apoptosis. We labeled proliferating cells and observed a significant increase in the percentage of Ki67⁺ cells in *Slit2*^{-/-};*Slit3*^{-/-}, compared with +/+, ducts (Fig. 1B). This increase is responsible for the excess cells

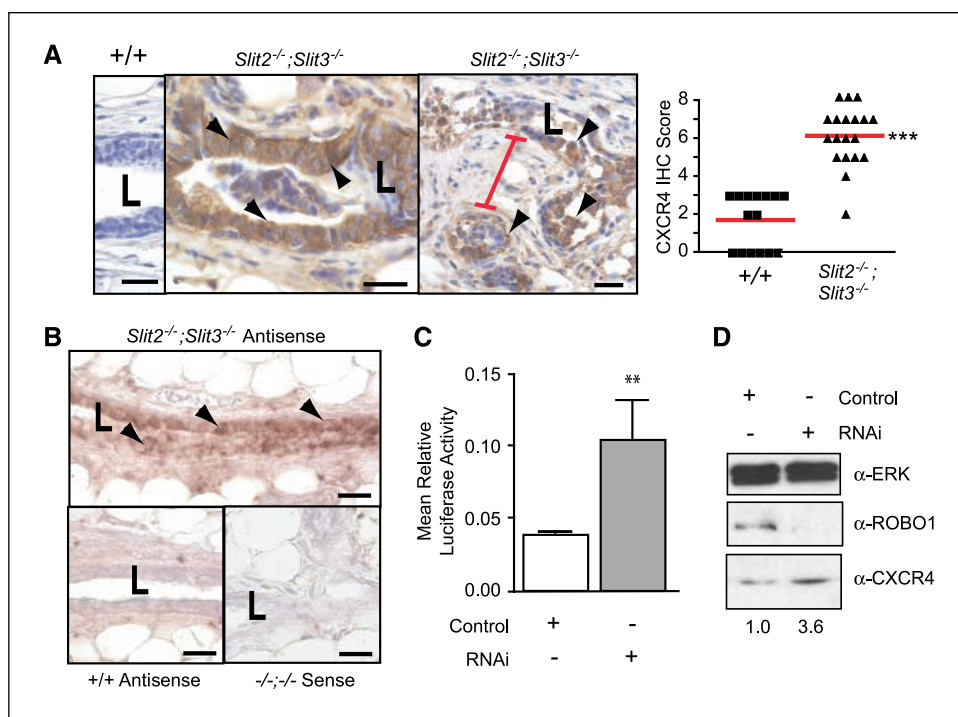


Figure 2. Loss of *Slit2* and *Slit3* causes up-regulation of CXCR4 in mouse mammary gland and human MCF7 cells. **A**, in *Slit2*^{-/-};*Slit3*^{-/-} outgrowths, CXCR4 protein expression is localized to epithelia, with desmoplastic stroma between lesions. Representative immunostaining with anti-CXCR4 on +/+ and *Slit2*^{-/-};*Slit3*^{-/-} mammary outgrowths. *Arrowheads*, positive epithelial cells. *Red bar*, condensed desmoplastic stroma. *Scale bar*, 20 μ m. CXCR4 immunostaining was scored according to positivity and staining intensity and plotted on a vertical scatter plot. *Red bars*, average score. Significantly more CXCR4 staining is seen in *Slit2*^{-/-};*Slit3*^{-/-} outgrowths. ***, *P* < 0.0001, Mann-Whitney. **B**, *Cxcr4* mRNA is specifically present in the epithelium of *Slit2*^{-/-};*Slit3*^{-/-} outgrowths. *In situ* hybridization on +/+ and *Slit2*^{-/-};*Slit3*^{-/-} outgrowths using antisense probes reveals *Cxcr4* mRNA in *Slit2*^{-/-};*Slit3*^{-/-}, but not +/+, cells. *Arrowheads*, positive epithelial cells. Sense probes show little or no background staining. *Scale bar*, 20 μ m. **L**, lumen. **C**, loss of SLIT/ROBO signaling in MCF7 cells leads to up-regulation of *Cxcr4* gene expression. Cells were treated with control or *Robo1* siRNA and then cotransfected with pGL-CXCR4(-375), which contains the *Cxcr4* promoter region coupled to the F-luciferase gene and pRL-TK (R-luciferase). Cells were lysed after 36 h and luciferase activity was measured in triplicate. Activities were normalized for transfection efficiency. *Columns*, mean relative luciferase activity; *bars*, SE. **, *P* = 0.0095, Mann-Whitney test. **D**, loss of SLIT/ROBO signaling in MCF7 cells leads to increased levels of CXCR4 protein. Representative immunoblots (*n* = 4). *Numbers*, CXCR4 band intensity.

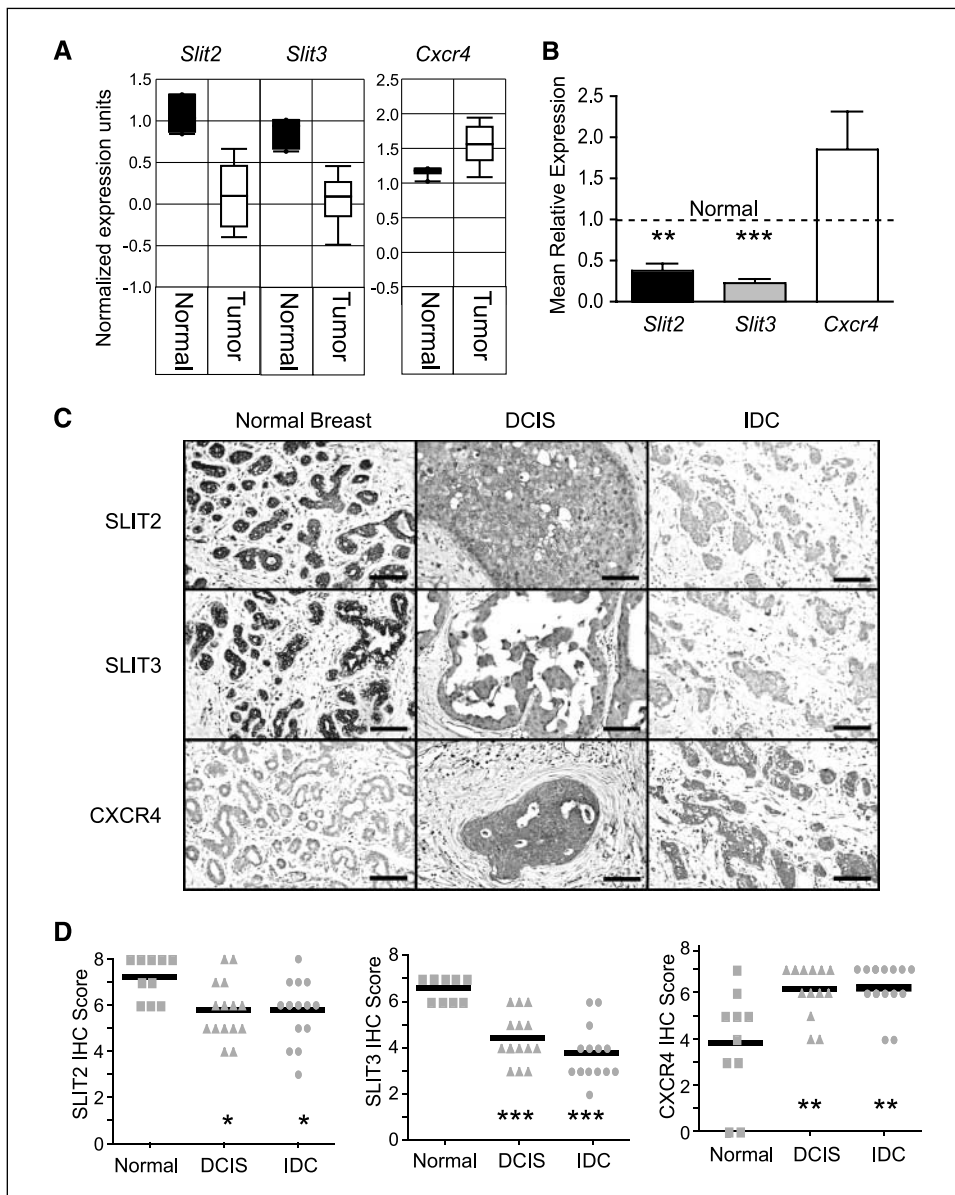


Figure 3. Loss of *Slit* expression in human tumors correlates with up-regulation of *Cxcr4*. **A**, box plots of data from the Richardson microarray data set were drawn using the OncoPrint Cancer Profiling Database (32). *Slit2* ($P = 2.6E-10$) and *Slit3* ($P = 7.1E-9$) expression is significantly reduced in tumors, whereas *Cxcr4* ($P = 1.8E-5$) expression is elevated. Normal, $n = 7$; tumor, $n = 40$; P values from t test. **B**, expression levels, by quantitative PCR, of *Slit2*, *Slit3*, and *Cxcr4* were obtained from a panel of tumors, with values normalized against internal control *GAPDH*. The data were then normalized to values obtained from normal breast ($n = 6$). A value of 1 equals expression level of the gene in average normal breast. Seventeen of 25 tumor samples (68%) showed elevated *Cxcr4* expression compared with normal breast. In these tumors, this elevation corresponded with significantly reduced expression of *Slit2* or *Slit3*. Columns, mean relative expression; bars, SE. *Slit2* versus *Cxcr4*: **, $P < 0.011$; *Slit3* versus *Cxcr4*: ***, $P < 0.001$, ANOVA. **C**, SLIT expression is decreased in tumors, whereas CXCR4 levels increase. Normal breast, DCIS, and IDC tissue sections were immunostained with anti-SLIT2, anti-SLIT3, and anti-CXCR4. Representative images are shown. Scale bar, 100 μ m. **D**, immunostained sections were scored according to cell percentage positivity and staining intensity. Scores were plotted on a vertical scatter plot. Black bars, average score. Both SLIT2 (*, $P = 0.01$, ANOVA) and SLIT3 (***, $P < 0.0001$, ANOVA) exhibit decreased expression in DCIS and IDC compared with normal breast. In contrast, CXCR4 is expressed at very low levels in normal breast, but its expression increases in DCIS and IDC (**, $P = 0.0005$, ANOVA).

because we evaluated apoptosis using activated caspase-3 staining and observed no difference (data not shown). Histopathologic analyses concurred with our observations that *Slit2*^{-/-};*Slit3*^{-/-} tissue contains hyperplasias. Condensed and desmoplastic stroma surrounding the lesions were also noted in the diagnosis (Fig. 1A), as was a large influx of immune infiltrates in the knockout, compared with wild-type, tissue.

ROBO1 is a SLIT receptor that could mediate the observed effects in the gland (23). *Robo1*^{-/-} animals are viable so we evaluated the loss-of-function phenotype using intact glands. Ducts in *Robo1*^{-/-} glands were hyperplastic and disorganized, displaying a phenotype that was indistinguishable from *Slit2*^{-/-};*Slit3*^{-/-} ductal lesions (Supplementary Fig. S1). As was the case for *Slit2*^{-/-};*Slit3*^{-/-} tissue, the penetrance of the phenotype was 100%, with ~30% of ducts displaying lesions that extended between 0.3 and 5.0 mm.

To investigate whether a similar phenotype occurred when SLIT/ROBO1 signaling was disrupted in human breast cells, we used the MCF7 line that retains several characteristics

of differentiated mammary epithelium, including expression of *Slit2*, *Slit3*, and *Robo1* (data not shown; ref. 31). Cells were treated with *Robo1* siRNA to down-regulate SLIT/ROBO1 signaling (Supplementary Fig. S2) and then cultured in Matrigel. MCF7 cells formed smooth, nonpolarized colonies without central lumens. In contrast, the siRNA-treated colonies were large and disorganized, a phenotype that was rescued by reexpression of *Robo1* (Fig. 1C). Immunostaining with Ki67 revealed a significantly higher fraction of proliferating cells in colonies treated with *Robo1* siRNA compared with control (Fig. 1D). This was similar to the elevated proliferation observed in *Slit2*^{-/-};*Slit3*^{-/-} outgrowths and *Robo1*^{-/-} glands (Fig. 1B; Supplementary Fig. S2). Together, these data show that a consequence of *Slit/Robo1* loss is elevated proliferation leading to hyperplastic lesions.

Loss of *Slit* up-regulates *Cxcr4* expression. We sought candidates whose misexpression in the absence of SLIT/ROBO1 signaling is responsible for the observed hyperplastic phenotype.

One candidate is CXCR4 because it is expressed early during breast tumorigenesis (1, 4), and blocking its expression or function inhibits breast tumor growth (8, 9). Western blots of whole gland lysates showed elevated CXCR4 expression in *Slit2*^{-/-};*Slit3*^{-/-}, compared with +/+, tissue (Supplementary Fig. S3). Immunohistochemistry revealed CXCR4 expression in a large fraction of cells in *Slit2*^{-/-};*Slit3*^{-/-} epithelium, with little or no expression in +/+

epithelium (Fig. 2A). We also observed condensed and desmoplastic stroma surrounding these CXCR4-positive lesions (Fig. 2A). Because CXCR4 is regulated by transcriptional and posttranscriptional mechanisms, we performed *in situ* hybridization studies and observed *Cxcr4* in *Slit* knockout, but not wild-type, epithelium (Fig. 2B). A transcriptional mechanism also occurred in *Robo1* siRNA-treated MCF7 cells because we observed increased *Cxcr4*

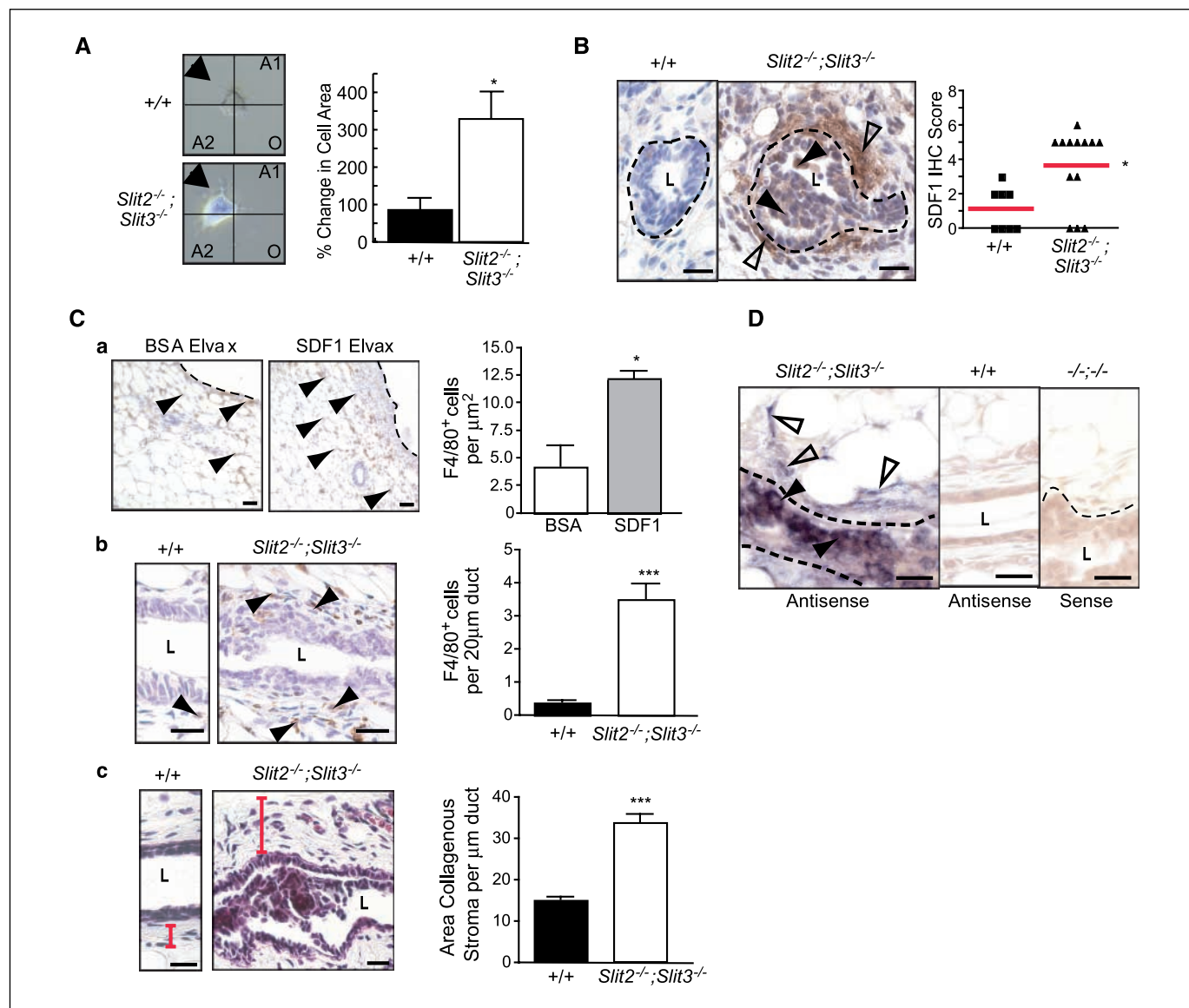


Figure 4. Loss of *Slit* expression results in coordinate up-regulation of SDF1 and the formation of desmoplastic stroma. **A**, *Slit2*^{-/-};*Slit3*^{-/-}, but not +/+, cells respond to a point source of SDF1. Primary epithelial cells were prepared from outgrowths and placed in stable liquid gradients of SDF1 (29). Phase-contrast images were acquired at 0 and 60 min. Using ImageJ, the change in cell area in the source quadrant (arrow) was calculated. Columns, mean percentage change ($n = 7$); bars, SE. *, $P = 0.0018$, Mann-Whitney. **B**, SDF1 protein is present in the stroma surrounding *Slit2*^{-/-};*Slit3*^{-/-} outgrowths. Representative immunostaining with anti-SDF1 on +/+ and *Slit2*^{-/-};*Slit3*^{-/-} mammary outgrowths. Dotted lines, epithelial/stromal interface. Open arrowheads, positive staining in stroma; arrowheads, epithelial cells expressing SDF1. Scale bar, 20 μm. SDF1 immunostaining was scored according to positivity and intensity. Scores were plotted on a vertical scatter plot. Red bars, average score. Significantly more SDF1 staining is seen in *Slit2*^{-/-};*Slit3*^{-/-} outgrowths. *, $P = 0.018$, Mann-Whitney. **C**, SDF1 attracts macrophages. **a**, representative images of F4/80 staining in fat pads containing BSA versus SDF1 Elvax pellets. The number of F4/80⁺ cells surrounding pellets was counted and expressed as the number of F4/80⁺ cells per μm². Columns, average; bars, SD. *, $P = 0.0086$, unpaired *t* test. Macrophages surround *Slit2*^{-/-};*Slit3*^{-/-} ducts. **b**, representative images of F4/80 staining in +/+ versus *Slit2*^{-/-};*Slit3*^{-/-} mammary outgrowths. Duct length was measured and the number of F4/80⁺ cells was counted (ImageJ software). Columns, average; bars, SD. *** $P < 0.0001$, unpaired *t* test ($n = 3$ animals, 10 fields of view/animal). Stroma surrounding *Slit2*^{-/-};*Slit3*^{-/-} ducts is desmoplastic. **c**, representative images of Masson's trichrome staining of +/+ versus *Slit2*^{-/-};*Slit3*^{-/-} tissue. Red bar, width of stroma. Longitudinal images of ducts were taken and duct length and positively stained areas were measured (ImageJ software). Columns, average; bars, SD. *** $P < 0.0001$, unpaired *t* test. Scale bar, 20 μm. **D**, *Sdf1* mRNA is specifically present in subpopulations of elongated stromal cells (open arrowheads) and epithelial cells (closed arrowheads) in *Slit2*^{-/-};*Slit3*^{-/-} outgrowths. *In situ* hybridization on +/+ and *Slit2*^{-/-};*Slit3*^{-/-} outgrowths using antisense probes reveals *Sdf1* mRNA in *Slit2*^{-/-};*Slit3*^{-/-}, but not +/+, cells. Sense probes show no or little background staining. Scale bar, 20 μm.

reporter gene activity and increased levels of CXCR4 in treated, compared with control, cells (Fig. 2C and D). Together, our results show that SLIT/ROBO1 signaling negatively regulates *Cxcr4* expression, with loss of this regulation leading to elevated levels of CXCR4 in murine tissue and human breast cancer cells.

If *Slits* silence *Cxcr4* in normal breast, we hypothesize that loss of *Slits* in tumors will correspond with elevated *Cxcr4*. To investigate, we analyzed microarray data sets from human breast tumor samples available at Oncomine.org (32) and found an inverse correlation between *Slit* and *Cxcr4* expression (Fig. 3A). We confirmed this by performing quantitative RT-PCR on a panel of human tumors; in 68% of tumors with elevated *Cxcr4* expression,

Slit2 or *Slit3* levels were significantly reduced compared with their expression in normal tissue (Fig. 3B). We further verified these observations at the protein level using immunohistochemistry on samples of normal breast, ductal carcinoma *in situ* (DCIS), and infiltrating ductal carcinoma (IDC; Fig. 3C and D). Again, there were robust levels of SLIT2 and SLIT3 in normal tissue that significantly decreased with increasing tumor grade. In contrast, and as previously shown (1, 4), little or no CXCR4 was detectable in normal breast, but its expression significantly increased with higher tumor grade.

Loss of *Slit* expression results in coordinate up-regulation of SDF1. Although CXCR4 is up-regulated in the vast majority of sampled premalignant lesions, studies on human breast cancer cell lines have suggested that it is only active in metastatic cells (33). To evaluate CXCR4 activity in *Slit2*^{-/-}; *Slit3*^{-/-} cells, we performed chemotaxis assays. *Slit2*^{-/-}; *Slit3*^{-/-} cells did not exhibit robust migration as expected of primary cells harvested from premalignant tissue but instead responded to SDF1 by reorganizing their cell membrane and sending membranous projections toward a point source (Fig. 4A). Wild-type cells were unresponsive to SDF1. This result suggested that CXCR4 expressed on *Slit2*^{-/-}; *Slit3*^{-/-} cells is active and reacts to its ligand.

This raised the question of whether SDF1 surrounded *Slit2*^{-/-}; *Slit3*^{-/-} lesions because recent studies have placed it in the tumor microenvironment (6, 7). We found abundant SDF1 expression in the epithelium and the surrounding stroma of knockout, but not wild-type, tissue (Fig. 4B). The presence of SDF1 is consistent with the histopathologic diagnosis that noted the infiltration of immune cells within desmoplastic stroma surrounding *Slit2*^{-/-}; *Slit3*^{-/-} lesions. Macrophages, which express CXCR4, represent a major component of immune infiltrates surrounding tumors and play a key role in promoting the angiogenic switch during malignant transition (34). To determine whether macrophages are attracted to SDF1, we implanted point sources of SDF1 or vehicle (BSA) into wild-type mammary glands (Fig. 4C, a). Significantly more macrophages (F4/80⁺) infiltrated into the tissue surrounding SDF1, compared with control, showing that SDF1 is a chemoattractant for macrophages and suggesting a role in recruiting these immune cells to tumors (Fig. 4C, a). Next, we

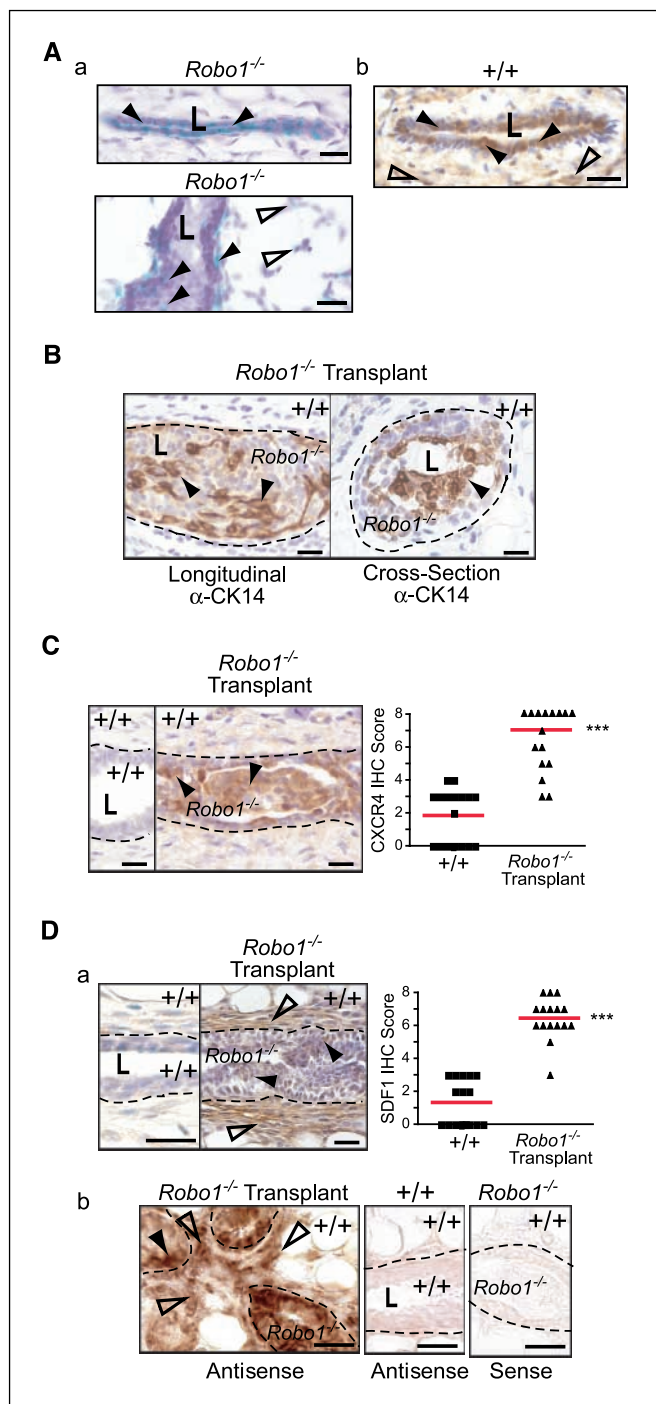
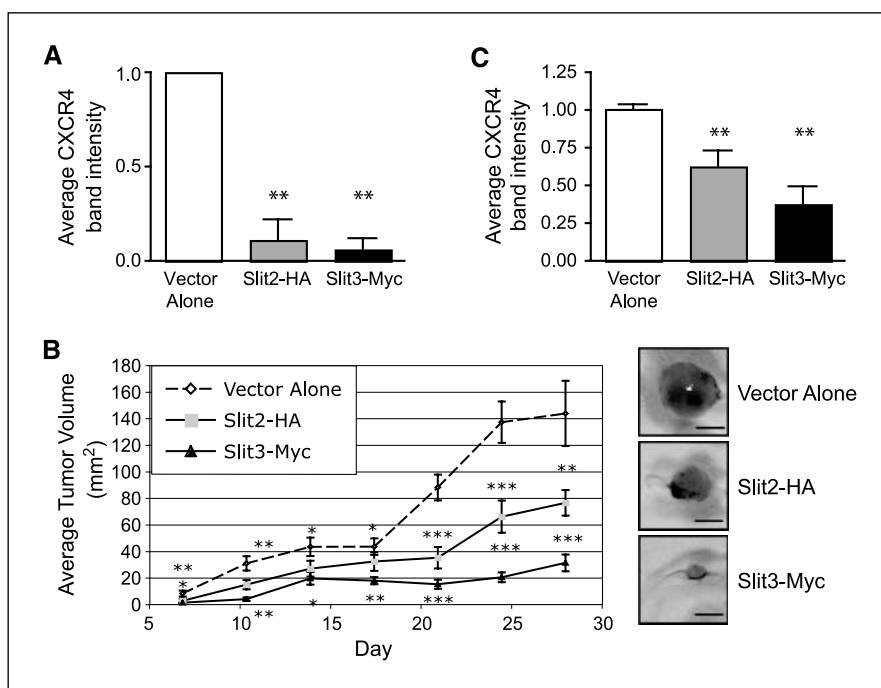


Figure 5. Coordinate up-regulation of CXCR4 and SDF1 is due to lack of SLIT/ROBO1 signaling within mammary epithelia. *A*, to examine *Robo1* gene expression, we took advantage of the *lacZ* gene under the control of the endogenous *Robo1* promoter in $-/-$ tissue. *a*, longitudinal sections of *Robo1*^{-/-} ducts stained for β -galactosidase activity. *b*, longitudinal section of +/+ duct immunostained with anti-ROBO1. Open arrows, positive stromal staining; arrowheads, positive epithelial cells. Scale bar, 20 μ m. *L*, lumen. *B*, transplanted *Robo1*^{-/-} mammary outgrowths show severe ductal defects similar to those observed in *Slit2*^{-/-}; *Slit3*^{-/-} outgrowths. Scale bar, 20 μ m. *C*, CXCR4 protein is specifically expressed in the epithelium of *Robo1*^{-/-} outgrowths. Representative immunostaining with anti-CXCR4 on +/+ stroma/+ epithelia and +/+ stroma/*Robo1*^{-/-} epithelia. Arrows, positive cells. Scale bar, 20 μ m. CXCR4 immunostaining was scored and plotted on a vertical scatter plot. Red bars, average score. Significantly more CXCR4 staining is seen in *Robo1*^{-/-} outgrowths. ***, $P < 0.0001$, Mann-Whitney test. *D*, SDF1 is present in the stroma surrounding *Robo1*^{-/-} epithelial outgrowths (*a*; open arrowheads) and in a subpopulation of epithelial cells (arrowheads). Representative immunostaining with anti-SDF1 on +/+ stroma/+ epithelia and +/+ stroma/*Robo1*^{-/-} epithelia. SDF1 immunostaining was scored and plotted on a vertical scatter plot. Red bars, average score. Significantly more SDF1 staining is seen in *Robo1*^{-/-} outgrowths. ***, $P < 0.0001$, Mann-Whitney test. *Sdf1* mRNA is present in subpopulations of stromal fibroblasts (*b*; open arrowheads) and epithelial cells (arrowheads) in *Robo1*^{-/-} outgrowths. *In situ* hybridization using +/+ stroma/+ epithelia and +/+ stroma/*Robo1*^{-/-} epithelia outgrowths using antisense probes reveals *Sdf1* mRNA in +/+ stroma/*Robo1*^{-/-} epithelia but not +/+ stroma/+ epithelia cells. Sense probes show little or no background staining. Scale bar, 20 μ m.

Figure 6. *Slit* expression in MDA-MB-231 cells blocks tumor growth by reducing CXCR4 expression. **A**, *Slit2*-HA and *Slit3*-Myc stable cell lines express low levels of CXCR4 compared with vector alone control lines. Stable *Slit2*-HA ($n = 3$) and *Slit3*-myc ($n = 2$) cell lines were generated by clonal selection. Stable cell line extracts were probed with anti-CXCR4. Columns, mean CXCR4 band intensity ($n = 2$ for each line); bars, SE. **, $P < 0.001$, ANOVA. **B**, expression of *Slit2* or *Slit3* resulted in smaller tumor size. Tumors were generated using *Slit* and control stable cell lines. $n = 12$ mice for each line. Points, mean tumor volume at each day; bars, SE. ***, $P < 0.0001$; **, $P < 0.001$; *, $P < 0.05$, ANOVA. Representative images of orthotopic tumors are shown. Scale bar, 0.25 mm. **C**, tumors expressing *Slit2* or *Slit3* contain significantly less CXCR4 protein compared with control tumors. Columns, mean CXCR4 immunoblot band intensity from $n = 3$ tumors; bars, SE. **, $P = 0.01$, ANOVA.



performed F4/80 immunohistochemistry on *Slit2*^{-/-}/*Slit3*^{-/-} and control tissue and found a significant increase in macrophages surrounding knockout tissue (Fig. 4C, b). We also evaluated the stromal expression of collagen, a major constituent of desmoplastic stroma (Fig. 4C, c). Stroma surrounding *Slit2*^{-/-}/*Slit3*^{-/-} epithelium contained significantly more condensed, collagenous stroma, compared with +/+, consistent with the histopathologic analysis. To define the cellular source of SDF1, we performed *in situ* hybridization analyses and discovered *Sdf1* in a fraction of epithelial cells and in a subset of elongated stromal cells that are likely to be fibroblasts based on their morphology (Fig. 4D). Thus, both CXCR4 and SDF1 are initially up-regulated in the epithelium, as has been recently observed in a xenograft model of DCIS (5). A local source of SDF1 may function to transform myoepithelial cells into CAFs or to recruit CAFs from circulating cells (35).

Epithelial regulation of CXCR4/SDF1 chemokine signaling axis. Together, the data show that loss of *Slit* expression leads to the coordinate up-regulation of *Cxcr4* in epithelia and *Sdf1* in both epithelia and stroma. This suggests that SLIT/ROBO1 signaling keeps SDF1/CXCR4 expression in check, but the regulatory networks may be complicated. *Slit* genes are expressed in the epithelia, but they encode a secreted cue that may act on any cell type expressing ROBO1 receptors. During mammary development, ROBO1 is expressed on myoepithelial cells (23), but as the gland matures, we observed a switch in its expression to include a subpopulation of luminal cells (Fig. 5A). ROBO1 was also expressed on stromal fibroblasts (Fig. 5A). Consequently, loss of *Slit* expression could regulate *Sdf1* and *Cxcr4* independently by disrupting ROBO1 signaling in both the stromal and epithelial compartments. Alternatively, loss of SLIT/ROBO1 signaling in just one compartment could up-regulate *Sdf1* and *Cxcr4* in both compartments.

To investigate, we eliminated SLIT/ROBO1 signaling selectively in the epithelial compartment by transplanting *Robo1*^{-/-} epithelium into wild-type stroma. In these chimeric glands, we observed disorganized, hyperplastic epithelial lesions (Fig. 5B), which

were similar in phenotype, penetrance (100%), and expressivity (19.64% ± SE 9.77; $n = 669$ ducts; 6 outgrowths) to those seen in *Slit2*^{-/-}/*Slit3*^{-/-} transplants (Fig. 1A). We evaluated the chemokine axis and again found up-regulation of CXCR4 in *Robo1*^{-/-} epithelium (Fig. 5C), and coordinate up-regulation of SDF1 in the surrounding +/+ stroma (Fig. 5D, a), which was desmoplastic and contained immune infiltrates similar to stroma surrounding *Slit2*^{-/-}/*Slit3*^{-/-} tissue (data not shown). These data show that loss of SLIT/ROBO1 signaling in the epithelial compartment, alone, up-regulates SDF1 and CXCR4. This leads to phenotypic changes similar to those occurring in *Slit2*^{-/-}/*Slit3*^{-/-} transplants in which SLIT/ROBO1 signaling is disrupted in both compartments. To define the source of SDF1 in the transplanted tissue, we performed *in situ* hybridization studies and found *Sdf1* mRNA in cell subpopulations in the epithelia and stroma (Fig. 5D, b), suggesting that loss of SLIT/ROBO1 signaling in breast epithelia at early stages of transformation both generates a local source of *Sdf1* and up-regulates *Cxcr4*. We therefore conclude that loss of SLIT/ROBO1 signaling in the epithelia, alone, is sufficient to drive the observed morphologic and molecular changes, resulting in hyperplastic lesions, surrounded by desmoplastic stroma.

SLITs suppress CXCR4 expression and inhibit tumor growth. Given that SLITs exert this regulatory function by inhibiting the expression of *Sdf1* and *Cxcr4* within the mammary epithelium, we wondered whether overexpression of *Slits* in human breast carcinoma cells would suppress *Cxcr4* expression and inhibit tumor growth. Previous studies have shown that the metastatic human cell line MDA-MB-231 expresses CXCR4, but not SDF1 (36), and that inhibiting CXCR4 expression or function in these cells blocks primary tumor growth (8, 9). Because MDA-MB-231 cells express ROBO1 and ROBO2 (21),⁴ signaling through these receptors could down-regulate CXCR4 expression and suppress tumor formation. To investigate, we transiently expressed *Myc-Slit2*

⁴ R. Marlow, unpublished data.

or *Myc-Slit3* in MDA-MB-231 cells and documented decreased CXCR4 expression (Supplementary Fig. S4). Next, we generated stable cell lines expressing *Slit2* ($n = 3$) or *Slit3* ($n = 2$) and again found reduced CXCR4 levels (Fig. 6A). We also observed that *Slit*-expressing cells formed significantly fewer colonies, compared with control, when cultured in Matrigel (Supplementary Fig. S5). This suggested a general inhibition of cell growth, so we pursued the observation by establishing orthotopic xenograft tumors in immunocompromised hosts. We found that *Slit*-expressing cells formed significantly smaller tumors over time, with *Slit3* producing the most dramatic effect (Fig. 6B). We confirmed sustained down-regulation of CXCR4 in *Slit*-expressing tumors after 28 days of *in vivo* incubation (Fig. 6C; Supplementary Fig. S6). Thus, expression of *Slits* in MDA-MB-231 cells both down-regulates CXCR4 and inhibits tumor growth. Together with the observation that targeting CXCR4 reduces tumor growth in numerous organs (37, 38), our results suggest that SLITs suppress tumor growth by inhibiting the proliferative consequences of elevated CXCR4 expression.

Discussion

There is extensive literature on the molecular and genetic alterations that occur in invasive breast carcinoma and signify poor prognosis, but relatively little progress has been made in defining the genetic changes occurring in premalignant lesions. Here, we report that loss of *Slit* expression early during tumor progression up-regulates a key chemokine signaling axis and generates hyperplastic changes in the epithelium, along with desmoplastic changes in the stroma. Expression of CXCR4 was originally thought to occur late during tumor progression, generating cells that are ready to metastasize and home to organs expressing high levels of SDF1 (3). This restricted view of CXCR4 function, however, has been called into question because 93% of studied cases of atypical ductal carcinoma display high levels of CXCR4 (4), suggesting a role for CXCR4 in mediating earlier aspects of cellular transformation. Our data show that changes, loss and gain, in *Slit* expression function as a switch in the epithelium that up-regulate and down-regulate *Cxcr4*, leading to attendant changes in proliferation. We also show that loss of *Slits* results in the coordinate up-regulation of *Sdf1* in both the epithelium and surrounding stroma and this is accompanied by changes in the local microenvironment consistent with transformation.

The importance of the tumor microenvironment is well established, but it is unclear how it is generated. Our studies show that loss of SLIT/ROBO1 signaling exclusively in the epithelia is sufficient to increase expression of both *Cxcr4* and *Sdf1* (Fig. 5). The establishment of an initial SDF1/CXCR4 signaling loop within the epithelium is supported by recent studies using human MCF10DCIS.com cells in a xenograft model (5). Both CXCR4 and SDF1 are expressed at low levels in early MCF10DCIS lesions. CXCR4 expression remains epithelial, but during intermediate stages of transformation, SDF1 is switched on in the activated stroma. Once the ductal carcinoma becomes invasive, SDF1 expression is extinguished in the epithelia and is exclusively expressed by CAFs in the activated stroma. The origin of these CAFs is currently unknown. Some may be transformed from normal fibroblasts by aberrant signals from cancerous epithelial cells, whereas others may be transformed after being recruited from circulating bone marrow-derived cells (35). In either case, the transformation of these cells seems to be a consequence of their

interaction with the cancerous epithelium. Our data raise the possibility that up-regulation of epithelial SDF1, accompanying *Slit* loss, contributes to the recruitment and/or transformation of CAFs, and support the model that genetic changes in the tumor epithelium, alone, are sufficient to drive transformation of cells and the surrounding microenvironment (7).

Our data also provide *in vivo* evidence that the SDF1/CXCR4 axis is fully functional within the epithelium during preinvasive stages of breast transformation and that it promotes cell survival and proliferation. We show that loss of SLIT/ROBO1 signaling results in the development of hyperplastic lesions (Fig. 1) with the coordinate up-regulation of both CXCR4 and SDF1 in the mammary epithelium (Figs. 2, 4, and 5). This type of autocrine stimulation of cell growth by SDF1/CXCR4 has been documented in human breast cancer cells on overexpression of SDF1 (39) and was also observed in the MCF10DCIS.com cells, described above, in which intraepithelial SDF1/CXCR4 signaling gives way to signaling across the epithelial/stromal boundary as the tumor microenvironment becomes established (5). Numerous pathways have been implicated in the mitogenic activity of SDF1/CXCR4 and may be responsible for the hyperplastic lesions observed in *Slit2*^{-/-};*Slit3*^{-/-} tissue (40). We are currently investigating the pathways that drive proliferation because targeting these pathways could provide therapies that arrest cellular proliferation in early stages of transformation.

The molecular mechanism through which cells acquire SDF1 and CXCR4 expression during the evolution of tumors is unclear. At later stages of cellular transformation, CXCR4 expression is up-regulated by several mechanisms (40). Our studies reveal a transcriptional mechanism during early stages of transformation that occurs within breast epithelia (Figs. 2, 4, and 5). We show that SLITs signal through their ROBO1 receptor to negatively regulate *Cxcr4* and *Sdf1*. Negative transcriptional regulation of both *Cxcr4* and *Sdf1* has been shown in renal cells where hypoxia-inducible factors 1 and 2 (Hif1 and Hif2) are targeted for degradation by von Hippel-Lindau (VHL) proteins (11). It has been shown that loss of VHL leads to stabilization of Hifs and subsequent up-regulation of both *Sdf1* and *Cxcr4* due to the Hif response elements contained in their promoters (41). Hifs are frequently up-regulated during breast transformation (42) and can drive the inappropriate proliferation of cells even under conditions of normal oxygen (43). Thus, Hifs or VHL proteins may be targeted by SLIT/ROBO1 signaling, and we are currently investigating their expression profiles in *Slit2*^{-/-};*Slit3*^{-/-} and *Robo1*^{-/-} glands.

Numerous studies show epigenetic inactivation of *Slits* in multiple types of cancer (15, 16, 18, 19), and in breast, this loss of *Slit* also correlates with increasing tumor grade (44). Our histopathologic analyses of *Slit2*^{-/-};*Slit3*^{-/-} and *Robo1*^{-/-} mammary epithelium revealed hyperplastic lesions with no nuclear atypia (Fig. 1), a type of lesion that can be found in ~30% of women with benign proliferative breast disease (45). Epidemiologic studies show that identification of such lesions confers a 2-fold increase in relative risk of developing invasive breast cancer compared with women without proliferative disease. For patients diagnosed with lesions having the next stage of severity, hyperplasias with nuclear atypia, the relative risk of future invasive disease rises to ~5-fold and increases to 10-fold if there is also positive family history (45, 46). These numbers show that, although most patients will not develop invasive disease, a fraction will. With medical advances enabling detection of breast lesions at earlier stages, it will be crucial to develop methods that distinguish between nascent disease and normal biology because current methods relying on

morphologic criteria are insufficient. Improved understanding of molecular signatures within breast lesions holds the promise of identifying those at high risk so they receive appropriate treatment while also identifying the majority who are not at risk so their medical concerns are dispelled (47). The findings presented in this report identify the loss of *Slit* expression as a marker of early lesions that have the potential to progress to invasive disease due to up-regulation of metastasis markers SDF1/CXCR4. We propose that these molecular alterations define a specific subclass of breast lesions whose early detection could lead to treatment strategies that prevent development of invasive disease.

Disclosure of Potential Conflicts of Interest

No potential conflicts of interest were disclosed.

References

- Salvucci O, Bouchard A, Baccarelli A, et al. The role of CXCR4 receptor expression in breast cancer: a large tissue microarray study. *Breast Cancer Res Treat* 2006;97:275–83.
- Holm NT, Byrnes K, Li BD, et al. Elevated levels of chemokine receptor CXCR4 in HER-2 negative breast cancer specimens predict recurrence. *J Surg Res* 2007; 141:53–9.
- Muller A, Homey B, Soto H, et al. Involvement of chemokine receptors in breast cancer metastasis. *Nature* 2001;410:50–6.
- Schmid BC, Rudas M, Reznicek GA, Leodolter S, Zeillinger R. CXCR4 is expressed in ductal carcinoma *in situ* of the breast and in atypical ductal hyperplasia. *Breast Cancer Res Treat* 2004;84:247–50.
- Tait LR, Pauley RJ, Santner SJ, et al. Dynamic stromal-epithelial interactions during progression of MCF10DCIS.com xenografts. *Int J Cancer* 2007;120: 2127–34.
- Orimo A, Gupta PB, Sgroi DC, et al. Stromal fibroblasts present in invasive human breast carcinomas promote tumor growth and angiogenesis through elevated SDF-1/CXCL12 secretion. *Cell* 2005;121:335–48.
- Allinen M, Beroukhi R, Cai L, et al. Molecular characterization of the tumor microenvironment in breast cancer. *Cancer Cell* 2004;6:17–32.
- Laptev N, Yang AG, Sanders DE, Strube RW, Chen SY. CXCR4 knockdown by small interfering RNA abrogates breast tumor growth *in vivo*. *Cancer Gene Ther* 2005;12:84–9.
- Smith MC, Luker KE, Garbow JR, et al. CXCR4 regulates growth of both primary and metastatic breast cancer. *Cancer Res* 2004;64:8604–12.
- Helbig G, Christopherson KW, Bhat-Nakshatri P, et al. NF- κ B promotes breast cancer cell migration and metastasis by inducing the expression of the chemokine receptor CXCR4. *J Biol Chem* 2003;278:21631–8.
- Staller P, Sulitkova J, Lisztwan J, Moch H, Oakeley EJ, Krek V. Chemokine receptor CXCR4 downregulated by von Hippel-Lindau tumour suppressor pVHL. *Nature* 2003;425:307–11.
- Lee BC, Lee TH, Zagazdzon R, Avraham S, Usheva A, Avraham HK. Carboxyl-terminal Src kinase homologous kinase negatively regulates the chemokine receptor CXCR4 through YY1 and impairs CXCR4/CXCL12 (SDF-1 α)-mediated breast cancer cell migration. *Cancer Res* 2005;65:2840–5.
- Li YM, Pan Y, Wei Y, et al. Upregulation of CXCR4 is essential for HER2-mediated tumor metastasis. *Cancer Cell* 2004;6:459–69.
- Hinck L. The versatile roles of "axon guidance" cues in tissue morphogenesis. *Dev Cell* 2004;7:783–93.
- Dallol A, Dickinson RE, Latif F. Epigenetic disruption of the SLIT-ROBO interactions in human cancer. In: Ablin RJ, Jiang WG, Esteller M, editors. DNA methylation, epigenetic and metastasis. New York: Springer Netherlands; 2005. p. 191–214.
- Narayan G, Goparaju C, Arias-Pulido H, et al. Promoter hypermethylation-mediated inactivation of

Acknowledgments

Received 4/16/2008; revised 6/30/2008; accepted 7/25/2008.

Grant support: American Cancer Society grant RSG0218001MGO, California Breast Cancer Research Program grant 10PB-0188, and National Cancer Institute grant R01CA128902 (L. Hinck) and Congressionally Directed Medical Research Program grant BC043200 and National Cancer Institute grant U01 CA105490 (R.D. Cardiff).

The costs of publication of this article were defrayed in part by the payment of page charges. This article must therefore be hereby marked advertisement in accordance with 18 U.S.C. Section 1734 solely to indicate this fact.

Santa Cruz Biotechnology generously provided antibodies and siRNA reagents. Other generous gifts were the following: anti-Dutt1 (Dr. Rabbitts, University College, London, United Kingdom), anti-HA (Dr. Doug Kellogg), MCF7 and MDA-MB-231 cell lines (Dr. Bissell, Lawrence Labs, Berkeley, CA), pGL-CXCR4(–375) (Dr. Avraham, Harvard Medical School, Boston, MA), pCRII-SDF1 (Dr. Goffinet, University of Louvain Medical School, Brussels, Belgium), pRL-TK (Dr. Haussler, University of California, Santa Cruz, CA), pSecTagB-*hSlit3*-C-myc (Dr. Roy Bicknell), *Slit3*^{–/–} mice (Dr. Ornitz, Washington University, St. Louis, MO), and *Slit2*^{–/–} mice and *Robo1*^{–/–} (Dr. Tessier-Lavigne, Genentech, Inc., South San Francisco, CA).

- multiple Slit-Robo pathway genes in cervical cancer progression. *Mol Cancer* 2006;5:16.
- Schmid BC, Reznicek GA, Fajjani G, Yoneda T, Leodolter S, Zeillinger R. The neuronal guidance cue Slit2 induces targeted migration and may play a role in brain metastasis of breast cancer cells. *Breast Cancer Res Treat* 2007;106:333–42.
- Latil A, Chene L, Cochant-Priollet B, et al. Quantification of expression of netrins, slits and their receptors in human prostate tumors. *Int J Cancer* 2003;103:306–15.
- Sharma G, Mirza S, Prasad CP, Srivastava A, Gupta SD, Ralhan R. Promoter hypermethylation of p16INK4A, p14ARF, CyclinD2 and Slit2 in serum and tumor DNA from breast cancer patients. *Life Sci* 2007;80:1873–81.
- Wu JY, Feng L, Park HT, et al. The neuronal repellent Slit inhibits leukocyte chemotaxis induced by chemotactic factors. *Nature* 2001;410:948–52.
- Prasad A, Fernandis AZ, Rao Y, Ganju RK. Slit protein-mediated inhibition of CXCR4-induced chemotactic and chemo-invasive signaling pathways in breast cancer cells. *J Biol Chem* 2004;279:9115–24.
- Chalasanani SH, Sabelko KA, Sunshine MJ, Littman DR, Raper JA. A chemokine, SDF-1, reduces the effectiveness of multiple axonal repellents and is required for normal axon pathfinding. *J Neurosci* 2003;23:1360–71.
- Strickland P, Shin GC, Plump A, Tessier-Lavigne M, Hinck L. Slit2 and netrin 1 act synergistically as adhesive cues to generate tubular bi-layers during ductal morphogenesis. *Development* 2006;133:823–32.
- Robinson GW, Accili D, Hennighausen L. Rescue of mammary epithelium of early lethal phenotypes by embryonic mammary gland transplantation as exemplified with insulin receptor null mice. New York: Kluwer Academic/Plenum Press; 2000. p. 307–16.
- Srinivasan K, Strickland P, Valdes A, Shin GC, Hinck L. Netrin-1/neogenin interaction stabilizes multipotent progenitor cap cells during mammary gland morphogenesis. *Dev Cell* 2003;4:371–82.
- Silberstein GB, Daniel CW. Investigation of mouse mammary ductal growth regulation using slow-release plastic implants. *J Dairy Sci* 1987;70:1981–90.
- Tissir F, Wang CE, Goffinet AM. Expression of the chemokine receptor Cxcr4 mRNA during mouse brain development. *Brain Res Dev Brain Res* 2004;149:63–71.
- Lee GY, Kenny PA, Lee EH, Bissell MJ. Three-dimensional culture models of normal and malignant breast epithelial cells. *Nat Methods* 2007;4:359–65.
- Bartoe JL, McKenna WL, Quan TK, et al. Protein interacting with C-kinase 1/protein kinase C α -mediated endocytosis converts netrin-1-mediated repulsion to attraction. *J Neurosci* 2006;26:3192–205.
- Wu X, Chen H, Parker B, et al. HOXB7, a homeodomain protein, is overexpressed in breast cancer and confers epithelial-mesenchymal transition. *Cancer Res* 2006;66:9527–34.
- Dallol A, Da Silva NF, Viacava P, et al. SLIT2, a human homologue of the *Drosophila Slit2* gene, has tumor suppressor activity and is frequently inactivated in lung and breast cancers. *Cancer Res* 2002;62:5874–80.
- Richardson AL, Wang ZC, De Nicolo A, et al. X

- chromosomal abnormalities in basal-like human breast cancer. *Cancer Cell* 2006;9:121–32.
- Holland JD, Kochetkova M, Akeawatchai C, Dottore M, Lopez A, McCol SR. Differential functional activation of chemokine receptor CXCR4 is mediated by G proteins in breast cancer cells. *Cancer Res* 2006;66:4117–24.
- Lin EY, Li JF, Gnatovskiy L, et al. Macrophages regulate the angiogenic switch in a mouse model of breast cancer. *Cancer Res* 2006;66:11238–46.
- Orimo A, Weinberg RA. Stromal fibroblasts in cancer: a novel tumor-promoting cell type. *Cell Cycle* 2006;5: 1597–601.
- Kang H, Watkins G, Parr C, Douglas-Jones A, Mansel RE, Jiang WG. Stromal cell derived factor-1: its influence on invasiveness and migration of breast cancer cells *in vitro*, and its association with prognosis and survival in human breast cancer. *Breast Cancer Res* 2005;7:R402–10.
- Rubin JB, Kung AL, Klein RS, et al. A small-molecule antagonist of SDF-1-CXCR4 inhibits intracranial growth of primary brain tumors. *Proc Natl Acad Sci U S A* 2003; 100:13513–8.
- De Falco V, Guarino V, Avilla E, et al. Biological role and potential therapeutic targeting of the chemokine receptor CXCR4 in undifferentiated thyroid cancer. *Cancer Res* 2007;67:11821–9.
- Kang H, Mansel RE, Jiang WG. Genetic manipulation of stromal cell-derived factor-1 attests the pivotal role of the autocrine SDF-1-CXCR4 pathway in the aggressiveness of breast cancer cells. *Int J Oncol* 2005;26:1429–34.
- Luker KE, Luker GD. Functions of CXCL12 and CXCR4 in breast cancer. *Cancer Lett* 2006;238:30–41.
- Zagzag D, Krishnamachary B, Yee H, et al. Stromal cell-derived factor-1 α and CXCR4 expression in hemangio-angioma and clear cell-renal cell carcinoma: von Hippel-Lindau loss-of-function induces expression of a ligand and its receptor. *Cancer Res* 2005;65:6178–88.
- Zhong H, De Marzo AM, Laughner E, et al. Overexpression of hypoxia-inducible factor 1 α in common human cancers and their metastases. *Cancer Res* 1999; 59:5830–5.
- Dang DT, Chen F, Gardner LB, et al. Hypoxia-inducible factor-1 α promotes nonhypoxia-mediated proliferation in colon cancer cells and xenografts. *Cancer Res* 2006;66:1684–936.
- Miller LD, Smeds J, George J, et al. An expression signature for p53 status in human breast cancer predicts mutation status, transcriptional effects, and patient survival. *Proc Natl Acad Sci U S A* 2005;102:13550–5.
- Hartmann LC, Sellers TA, Frost MH, et al. Benign breast disease and the risk of breast cancer. *N Engl J Med* 2005;353:229–37.
- Fitzgibbons PL, Henson DE, Hutter RV. Benign breast changes and the risk for subsequent breast cancer: an update of the 1985 consensus statement. Cancer Committee of the College of American Pathologists. *Arch Pathol Lab Med* 1998;122:1053–5.
- Jeffrey SS, Pollack JR. The diagnosis and management of pre-invasive breast disease: promise of new technologies in understanding pre-invasive breast lesions. *Breast Cancer Res* 2003;5:320–8.